ELEMENTARY EXCITATION OF THE BIMODAL ISING SPIN GLASS ON A SQUARE LATTICE

NOPARIT JINUNTUYA

A THESIS SUBMITTED IN PARTIAL FULFILLMENT
OF THE REQUIREMENTS FOR
THE DEGREE OF DOCTOR OF PHILOSOPHY
(PHYSICS)
FACULTY OF GRADUATE STUDIES
MAHIDOL UNIVERSITY
2013

Thesis

entitled

ELEMENTARY EXCITATION OF THE BIMODAL ISING SPIN GLASS ON A SQUARE LATTICE

.....

Mr. Noparit Jinuntuya
Candidate

.....

Prof. Julian Poulter,
Ph.D. (Physics)
Major advisor

.....

Prof. I-Ming Tang,
Ph.D. (Physics)
Co-advisor

.....

Prof. Suthat Yoksan,
Ph.D. (Physics)
Co-advisor

.....

Prof. Banchong Mahaisavariya,
M.D., Dip Thai Board of Orthopedics
Dean
Faculty of Graduate Studies
Mahidol University

.....

Asst. Prof. Narin Nuttavut,
Ph.D. (Physics)
Program Director
Doctor of Philosophy Program
in Physics
Faculty of Science
Mahidol University

Thesis

entitled

ELEMENTARY EXCITATION OF THE BIMODAL ISING SPIN GLASS ON A SQUARE LATTICE

was submitted to the Faculty of Graduate Studies, Mahidol University
for the degree of Doctor of Philosophy (Physics)
on
May 2, 2013

.....
Mr. Nopparit Jinuntuya
Candidate

Wanyok Atisattapong
.....
Lect. Wanyok Atisattapong,
Ph.D. (Mathematics)
Chair

.....
Prof. Julian Poulter,
Ph.D. (Physics)
Member

Suthat Yoksan
.....
Prof. Suthat Yoksan,
Ph.D. (Physics)
Member

.....
Prof. I-Ming Tang,
Ph.D. (Physics)
Member

B. Mahaisavariya
.....
Prof. Banchong Mahaisavariya,
M.D., Dip Thai Board of Orthopedics
Dean
Faculty of Graduate Studies
Mahidol University

.....
Prof. Skorn Mongkolsuk,
Ph.D. (Biological Science)
Dean
Faculty of Science
Mahidol University

ACKNOWLEDGEMENTS

I would like to express my deep appreciation to my thesis advisor, Prof. Julian Poulter, for his supervision and encouragement throughout this research. It has been very pleasure to work with him. He is a role model to me for how a good physicist should be.

I am also very grateful to my co-advisors, Prof. I-Ming Tang and Prof. Suthat Yoksan, for their thoughtful comments. My appreciation is also expressed to Dr. Wanyok Atisattapong, my external committee, for her comments

I wish to thanks the Ministry of Science and Technology for the scholarship which enabled me to undertake this study.

I am very appreciated for help and support from my colleagues. I express my special thanks to Dr. Wiwat Wongkorkour, Head of the Department of Physics, Kasetsart University, for his kindness to allow me to use the department Rock Cluster for my research. I would like to thanks the staffs in the Department of Physics, Mahidol University, for their help and support. A special thanks is expressed to Busara Pattanasiri for her help in the final stage of this thesis preparation.

Last but not least, I express my sincere gratitude to my family for their patience, encouragement and support throughout my long study.

Noparit Jinuntuya

ELEMENTARY EXCITATION OF THE BIMODAL ISING SPIN GLASS ON A SQUARE LATTICE

NOPARIT JINUNTUYA 5037478 SCPY/D

Ph.D. (PHYSICS)

THESIS ADVISORY COMMITTEE: JULIAN POULTER, Ph.D., I-MING TANG, Ph.D., SUTHAT YOKSAN, Ph.D.

ABSTRACT

In this thesis we investigate the energy gap of the bimodal Ising spin glass model on a square lattice. We study systems with periodic boundary conditions in one direction, embedded in an infinite ferromagnetic nest in the second direction. The Pfaffian method and degenerate state perturbation theory are used to calculate the degeneracies of the low-lying states. The existence of an energy state can be determined from the non-zero value of its degeneracy. We find that energy gaps depend strongly on the defect concentration and the system size. In the ferromagnetic phase, the energy gap is 4*J*, no matter what the system size is. In the spin glass phase, on the contrary, the energy gap is 2*J* when the system size *L* is odd, while it is 4*J* when *L* is even. For the system with odd *L*, finite size scaling analysis suggests to us that there is a sharp transition concentration p_c = 0.1045(11) where 2*J* excitations start to exist. This value of pc agrees well with the ferromagnetic-spin glass transition concentration found in the literature. We find that the 2*J* excitations are involved with spins across the system. We expect that these spanning excitations are a characteristic of the spin glass phase. We also investigate the distributions of the degeneracies of the 2*J* and 4*J* states, and find that they develop fat tails when *L* is increasing. Sample-to-sample fluctuations of the distributions suggest to us that we cannot expect that the first excited states will dominate the low temperature heat capacity. Elementary excitations of the spin glass model are not represented by the energy gap, and should involve many (if not all) excited states.

KEY WORDS: ±*J* ISING SPIN GLASS / ELEMENTARY EXCITATION ENERGY GAP / EXCITED STATE / PHASE TRANSITION

52 pages

การกระตุ้นมูลฐานของแบบจำลองไอซิงสปินกลาส แบบทวิฐานนิยม บนโครงผึกรูปสี่เหลี่ยมจัตุรัส
ELEMENTARY EXCITATION OF THE BIMODAL ISING SPIN GLASS ON A SQUARE LATTICE

นพฤทธิ์ จินันทุยา 5037478 SCPY/D

ปร.ด. (ฟิสิกส์)

คณะกรรมการที่ปรึกษาวิทยานิพนธ์: จูเลี่ยน พอลเตอร์, Ph.D., อี๊ มิน ถัง, Ph.D., สุทัศน์ ยกส้าน Ph.D.

บทคัดย่อ

ในวิทยานิพนธ์ฉบับนี้ เราได้ศึกษาช่องว่างพลังงานในแบบจำลองไอซิงสปินกลาส แบบทวิฐานนิยม บนโครงผึกรูปสี่เหลี่ยมจัตุรัส เราได้ศึกษาระบบที่มีเงื่อนไขขอบแบบเป็นคาบในทิศทางหนึ่ง และเงื่อนไขขอบแบบฝังตัวในโครงข่ายแม่เหล็กเฟโรขนาดอนันต์ในอีกทิศทางหนึ่ง ระเบียบวิธีฟัฟเฟียน และทฤษฎีเพอร์เทอร์เบชันสำหรับระบบที่มีสถานะซ้ำ ถูกใช้เพื่อคำนวณจำนวนซ้ำของสถานะพลังงานในระดับต่ำ การมีอยู่ของสถานะพลังงานสามารถพิจารณาได้จากจำนวนซ้ำที่มากกว่าศูนย์ของสถานะนั้นๆ เราพบว่าขนาดของช่องว่างพลังงานขึ้นอยู่เป็นอย่างยิ่งกับความเข้มข้นของสิ่งเจือและขนาดของระบบ ในสถานะแม่เหล็กเฟโร ช่องว่างพลังงานจะมีค่าเท่ากับ $4J$ โดยไม่ขึ้นกับขนาดของระบบ ตรงกันข้าม ในสถานะสปินกลาส ช่องว่างพลังงานมีค่าเท่ากับ $2J$ เมื่อขนาดของระบบ L เป็นจำนวนคี่ และมีค่าเป็น $4J$ เมื่อ L เป็นจำนวนคู่ จากการวิเคราะห์สเกลลิ่งขนาดจำกัด กับระบบที่ L เป็นจำนวนคี่ ชี้ว่า สถานะพลังงาน $2J$ จะเกิดขึ้นอย่างทันทีทันใด เมื่อความเข้มข้นของสิ่งเจือ $p_c = 0.0145(11)$ ค่า p_c นี้ สอดคล้องเป็นอย่างดีกับค่าความเข้มข้นที่เกิดการเปลี่ยนสถานะแม่เหล็กเฟโรกับสปินกลาส ที่พบในเอกสารการศึกษาอื่นๆ เราพบด้วยว่าสถานะกระตุ้น $2J$ เกี่ยวข้องกับสปินทั้งระบบ เราเชื่อว่าการกระตุ้นที่กระจายทั้งระบบเช่นนี้ เป็นลักษณะสมบัติของสถานะสปินกลาส เรายังได้ศึกษาการแจกแจงของจำนวนซ้ำของสถานะ $2J$ และ $4J$ และพบว่า การแจกแจงจะมีหางที่หนาขึ้นเมื่อ L เพิ่มขึ้น การกระเพื่อมของการแจกแจงจากตัวอย่างหนึ่งสู่อีกตัวอย่างหนึ่งชี้ให้เห็นว่า เราไม่อาจคาดว่าสถานะกระตุ้นที่หนึ่งจะเป็นปัจจัยสำคัญหลักในการกำหนดค่าความร้อนจำเพาะที่อุณหภูมิต่ำ การกระตุ้นมูลฐานในแบบจำลองสปินกลาสไม่ใช่ขนาดของช่องว่างพลังงาน แต่เกี่ยวข้องกับสถานะกระตุ้นจำนวนมาก (หรือทั้งหมด)

52 หน้า

CONTENTS

CONTENTS (cont.)

LIST OF FIGURES

LIST OF FIGURES (cont.)

LIST OF FIGURES (cont.)

LIST OF FIGURES (cont.)

CHAPTER I
INTRODUCTION

1.1 Introduction to Spin Glass Model

The term spin glass refers to the complex behaviour of systems subject to quenched disorder and frustration due to competition of mixed interactions. The name was first coined in the late 1960's by B. R. Coles to identify a class of magnetic alloys [1]. The pioneering studies were on CuMn and AuFe, with finite concentrations of the magnetic ions Mn or Fe in the non-magnetic hosts Cu and Au. The reason for the name spin glass is that in the disordered state the magnetic moments, or spins, on the magnetic ions seem to freeze in orientation but without any periodic ordering. This is conceptually similar to the amorphous freezing of the locations of atoms in a conventional (structural) glass.

Since its discovery, attempts have been made to understand this complex system, both theoretically and experimentally. On the theoretical side, much effort has gone into studies of a simplified model that grabs the essential ingredients of the real spin glass. It was proposed by S. F. Edwards and P. W. Anderson that the key features of these complex systems are the quenched disorder and frustration due to the mixed ferromagnetic and antiferromagnetic interactions. They also introduced a simple model that includes these important features, which is known as the Edward-Anderson (or EA) model [2]. Since then, there have been a lot of studies to understand the properties of this model and its variants. It is interesting that most studies are not motivated by promising new materials, but from the desire for a deep understanding of the complexity of the disordered system. This model has a wide range of applications, from magnetic alloys to biological systems, hard optimization to information theory, and financial analysis to social science. Some reviews of spin glass theory and applications can be found in [1,3–7].

The model studied in this thesis is the bimodal, or $\pm J$, Ising spin glass on a $L \times L$ square lattice. It is an EA model with the hamiltonian

$$H = -\sum_{\langle ij \rangle} J_{ij} s_i s_j , \tag{1.1}$$

where the sum is over all nearest neighbour pairs. The spin variables s_i take the values ±1. The random interaction J_{ij} has a fixed magnitude J but with random sign and probability distribution

$$P(J_{ij}) = p\,\delta(J_{ij} + J) + (1-p)\,\delta(J_{ij} - J). \tag{1.2}$$

The concentration p of negative, or antiferromagnetic, bonds is varied from zero up to the canonical spin glass at $p = 0.5$. It is believed that the spin glass can only exist at zero temperature [8] where $p > p_c$ with $p_c \approx 0.103$ [9–11].

1.2 Statement of the Problems

1.2.1 Existence of 2*J* Excitations

The low temperature properties of the model are not fully understood. The issues that interest us in this thesis are the energies and distributions of low-lying states. There are long debates about the value of the energy gap of the system. First, let us consider an Ising model with pure ferromagnetic interactions. It is obvious that, on the infinite system, the energy gap between the first excited states and the ground states is 8*J*. Once we introduce the antiferromagnetic bonds, one may expect that the energy gap is 4J. This can be achieved, for example, by flipping a spin, as shown in figure 1.1.

Nevertheless, for a finite system 2*J* excitations are possible. For the system with an open boundary the 2*J* excitations can be obtained simply by flipping a spin on the boundary, as shown in figure 1.2. Flipping a set of spins involving the boundary also gives 2*J* excitations. An example is shown in figure 1.3. However, we are particularly interested in the spanning 2*J* excitations, which involve flipping a set of spins on one side of some path that spans across the system. Figure 1.4 shows an example. This kind of excitation is quite interesting. It involves spins across the system. It also depends strongly on the concentration of the antiferromagnetic bonds. When the concentration is low, it is hard to find a spanning path that, when all spins on

one side are flipped, gives an excitation as low as $2J$. On the other hand if the concentration is high enough, we may expect that such a path can be easily found.

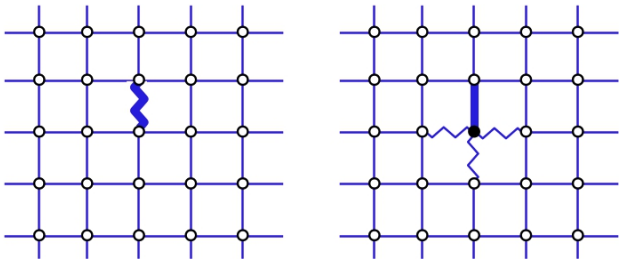

Figure 1.1: An example of a $4J$ excitation. In this system every bond is ferromagnetic (thin lines) except one bond in the middle which is antiferromagnetic (thick lines). White dots represent spin up and black dots represent spin down. Jagged lines represent unsatisfied bonds. On the left is a ground state configuration with one unsatisfied bond. On the right is a first excited state obtained by flipping a spin. The excited state has three unsatisfied bonds. The energy difference is thus $4J$.

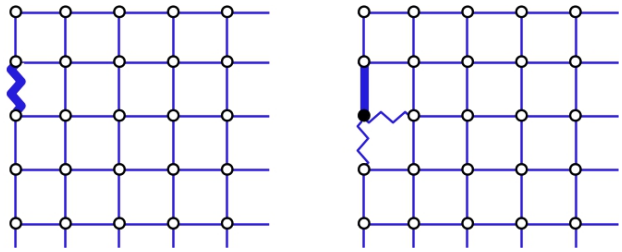

Figure 1.2: An example of a $2J$ excitation. A spin on the open boundary is flipped. The number of unsatisfied bonds is increased from one to two and the energy difference is $2J$.

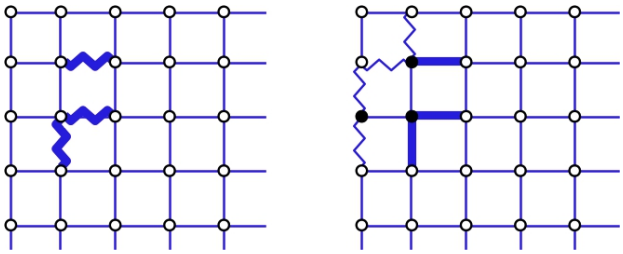

Figure 1.3: Another example of a $2J$ excitation. Three spins, with one spin on the boundary, are flipped. The number of unsatisfied bonds is increased from three to four, thus the energy difference is $2J$.

We believe that these spanning 2*J* excitations are the signature of the spin glass phase. It is interesting to see whether or not there is a sharp transition between two phases where the 2*J* excitations do not and do exist in the thermodynamic limit. It is even more interesting to see that whether this transition concentration coincides with the ferromagnetic-spin glass transition p_c or not.

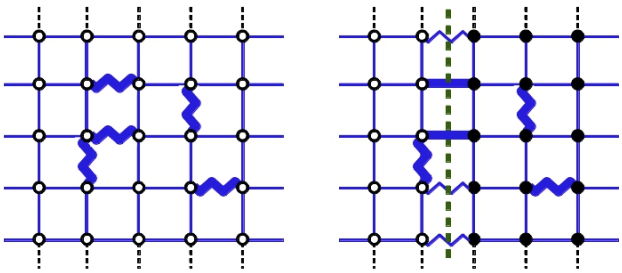

Figure 1.4: An example of spanning 2*J* excitation. On the left is a ground state configuration with five unsatisfied bonds. On the right is a first excited state obtained by flipping all spins on one side of the vertical broken line. The excited state has six unsatisfied bonds.

In principle, we may tackle this problem geometrically, although this is impractical for a large system. There is an exact algorithm to calculate the degeneracies of excited states [12]. It is practical to detect the spanning 2*J* excitations by measuring their degeneracies. However, in the open boundary system, there also exist local 2*J* excitations, as shown in figures 1.2 and 1.3. To focus on the spanning 2*J* excitations only, it is more convenient to work with an alternative boundary condition. We study the system with periodic boundary conditions in one direction, embedded in an infinite ferromagnetic nest in the second direction. We may have spanning 2*J* excitations if the linear dimension *L* in the direction of the periodic boundary is odd. These 2*J* excitations involve flipping all spins on one side of some closed path wrapping around the system. Figure 1.5 shows an example. Other closed paths can give excitations with energies equal to an odd multiple of 2*J*. There are no local (not spanning) 2*J* excitations in this system. Where the degeneracy of the 2*J* states is greater than zero, the spanning 2*J* excitations exist.

1.2.2 Distributions of Low-Lying States

Working with periodic-nested boundary conditions gives rise to the second issue of this thesis. It was shown [12] that if L is even, 2*J* excitations are not allowed. The closed paths give 4*J* excitations and the energy gap is 4*J*. For a system with full periodic boundary conditions (both directions), the spanning excitations need two closed paths and the energy gap is thus 4*J*. We now come to the situation that the size of the energy gap depends on the boundary conditions. This behaviour contradicts the requirement that physical quantities should be independent of boundary condition in the thermodynamic limit.

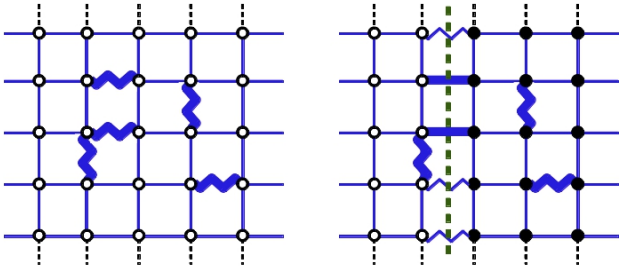

Figure 1.5: An example of a 2*J* excitation in the system with periodic boundary conditions in the *x*-direction and embedded in an infinite ferromagnetic nest in the *y*-direction. On the left is a ground state configuration with five unsatisfied bonds. On the right is a first excited state obtained by flipping all spins on one side of the vertical broken line. The excited state has six unsatisfied bonds.

We believe that these strange behaviours are closely related to the controversy of the low temperature thermal response, that is the specific heat, of the model. In the bimodal spin glass, since the energy levels are discrete, the partition function can be written as the sum over energy states of the Boltzmann weights

$$Z = 2 M_0 e^{-\frac{E_0}{kT}} \left(1 + \frac{M_1}{M_0} e^{-\frac{\Delta E_1}{kT}} + \frac{M_2}{M_0} e^{-\frac{\Delta E_2}{kT}} + \cdots \right) \tag{1.3}$$

where $\Delta E_i = E_i - E_0$. E_0 is the ground state energy and E_i is the energy of the *i*th excited state. M_0 is the ground state degeneracy and M_i is the degeneracy of the *i*th excited state. The factor 2 comes from global inversion. Using thermodynamic relations

$F = -kT \ln Z$, $S = -\frac{dF}{dT}$ and $E = F + TS$ together with the expansion $\ln(1+x) = x - \frac{x^2}{2} + \frac{x^3}{3} - \cdots$, we can write the specific heat as

$$\begin{aligned} c_v &= \frac{1}{L^2}\frac{dE}{dT} \\ &= \frac{1}{k(LT)^2}\left\{ \Delta E_1^2 \frac{M_1}{M_0} e^{-\frac{\Delta E_1}{kT}} + \Delta E_2^2 \left[\frac{M_2}{M_0} - \frac{1}{2}\left(\frac{M_1}{M_0}\right)^2 \right] e^{-\frac{\Delta E_2}{kT}} + \cdots \right\} \end{aligned} \tag{1.4}$$

Note that, since the above expansion of $\ln(1 + x)$ is valid only when $x < 1$, the relation for c_v is valid at low temperature only. If the temperature is low enough, we may naively expect that the first term dominates the series and the low temperature specific heat varies with the temperature as

$$c_v \sim \frac{E_g^2}{k(LT)^2}\frac{M_1}{M_0}\exp\left(-\frac{E_g}{kT}\right). \tag{1.5}$$

where $E_g = \Delta E_1$ is the energy gap. To get this relation we implicitly assume that the distribution of the ratio M_1/M_0 is sharp and we expect a definite value in the thermodynamic limit. However, it was found [12] that, for the canonical spin glass with even L, the distributions of the degeneracies of the low-lying states are broad and have fat tails, especially with increasing L. This means that we cannot assume the functional form of cv in equation 1.5. Even though there is an energy gap, saying that the ground states and first excited states dominate the low temperature physics may not be physically meaningful. For a finite system, we cannot lower the temperature beyond the point where ground states and first excited states start dominating the behaviour of the system.

Recently, there is a report [13] that the specific heat varies as a power law with the temperature. Since the calculations are performed for very large systems, this result is very reliable. The calculations are based on the assumption that the low temperature specific heat contains contributions from excitations having a range of energies. This idea seems to fit well with the discussion above that the low temperature physics may be not affected by the energy gap. The power law scaling of specific heat is similar to that of the Gaussian model, where the random interaction J_{ij}

is Gaussian distributed. It seems that in the thermodynamic limit the bimodal Ising spin glass model in two dimensions is “gapless” as in the Gaussian model.

For the second issue of this thesis, we want to show that broad distributions of the degeneracies of the low-lying states are also the characteristic of the spin glass phase. We believe that the broad distributions result from the existence of the spanning excitation paths. In the ferromagnetic phase, there are no spanning $2J$ paths in the thermodynamic limit. The energy gap should be $4J$, regardless of the boundary conditions. Since it is reasonable to expect that there are no spanning $4J$ paths either, the distributions of $4J$ states should be sharp. On the contrary, in the spin glass phase we can expect a lot of spanning paths, and the distributions of low-lying states should be broad.

To show this, we investigate the distributions of the low-lying energy states of the systems with the nested-periodic boundary condition, just above and below the critical concentration p_c. We believe that the results should reflect the characteristics of the other boundary conditions. We adapt the algorithm in [12,14] to calculate the degeneracies of the excited states for large numbers of disorder realisations. We then use a sophisticated algorithm to estimate the distributions of the degeneracies. The shape of distributions for both phases are then investigated. For the systems with odd L, the distributions of $2J$ states above and below p_c are compared. For the systems with even L, we investigate the distributions of $4J$ states. For comparison, we also investigate the distributions of $4J$ states for the system with odd L.

1.3 Objectives and Outline of the Thesis

In this thesis we propose to:

- Investigate the existence of spanning $2J$ excitations in the bimodal Ising spin glass model on a square lattice with periodic boundary conditions in one direction, embedded in an infinite ferromagnetic nest in the second direction, and odd L.

- Estimate the transition concentration that separates the two phases where the $2J$ excitations do not and do exist in the thermodynamic limit. Examine whether this coincides with the ferromagnetic-spin glass transition p_c or not.

- Investigate the distributions of low-lying states. Compare the shapes of the distributions above and below p_c. Examine whether a broad distribution is characteristic of the spin glass phase or not.

The detail of the our studies is given in the following chapters. After this introductory chapter, we review the related literature in chapter 2. The existence of $2J$ excitations, the mathematical formalism, and the computer algorithms used in our analyses are described in chapter 3. The results and discussion are then given in chapter 4. Chapter 5 summarises what we have done and introduces some interesting issues for further study.

CHAPTER I
INTRODUCTION

1.1 Introduction to Spin Glass Model

The term spin glass refers to the complex behaviour of systems subject to quenched disorder and frustration due to competition of mixed interactions. The name was first coined in the late 1960's by B. R. Coles to identify a class of magnetic alloys [1]. The pioneering studies were on CuMn and AuFe, with finite concentrations of the magnetic ions Mn or Fe in the non-magnetic hosts Cu and Au. The reason for the name spin glass is that in the disordered state the magnetic moments, or spins, on the magnetic ions seem to freeze in orientation but without any periodic ordering. This is conceptually similar to the amorphous freezing of the locations of atoms in a conventional (structural) glass.

Since its discovery, attempts have been made to understand this complex system, both theoretically and experimentally. On the theoretical side, much effort has gone into studies of a simplified model that grabs the essential ingredients of the real spin glass. It was proposed by S. F. Edwards and P. W. Anderson that the key features of these complex systems are the quenched disorder and frustration due to the mixed ferromagnetic and antiferromagnetic interactions. They also introduced a simple model that includes these important features, which is known as the Edward-Anderson (or EA) model [2]. Since then, there have been a lot of studies to understand the properties of this model and its variants. It is interesting that most studies are not motivated by promising new materials, but from the desire for a deep understanding of the complexity of the disordered system. This model has a wide range of applications, from magnetic alloys to biological systems, hard optimization to information theory, and financial analysis to social science. Some reviews of spin glass theory and applications can be found in [1,3–7].

The model studied in this thesis is the bimodal, or $\pm J$, Ising spin glass on a $L \times L$ square lattice. It is an EA model with the hamiltonian

$$H = -\sum_{\langle ij \rangle} J_{ij} s_i s_j , \tag{1.1}$$

where the sum is over all nearest neighbour pairs. The spin variables s_i take the values ±1. The random interaction J_{ij} has a fixed magnitude J but with random sign and probability distribution

$$P(J_{ij}) = p\,\delta(J_{ij} + J) + (1-p)\,\delta(J_{ij} - J). \tag{1.2}$$

The concentration p of negative, or antiferromagnetic, bonds is varied from zero up to the canonical spin glass at $p = 0.5$. It is believed that the spin glass can only exist at zero temperature [8] where $p > p_c$ with $p_c \approx 0.103$ [9–11].

1.2 Statement of the Problems

1.2.1 Existence of 2*J* Excitations

The low temperature properties of the model are not fully understood. The issues that interest us in this thesis are the energies and distributions of low-lying states. There are long debates about the value of the energy gap of the system. First, let us consider an Ising model with pure ferromagnetic interactions. It is obvious that, on the infinite system, the energy gap between the first excited states and the ground states is 8*J*. Once we introduce the antiferromagnetic bonds, one may expect that the energy gap is 4J. This can be achieved, for example, by flipping a spin, as shown in figure 1.1.

Nevertheless, for a finite system 2*J* excitations are possible. For the system with an open boundary the 2*J* excitations can be obtained simply by flipping a spin on the boundary, as shown in figure 1.2. Flipping a set of spins involving the boundary also gives 2*J* excitations. An example is shown in figure 1.3. However, we are particularly interested in the spanning 2*J* excitations, which involve flipping a set of spins on one side of some path that spans across the system. Figure 1.4 shows an example. This kind of excitation is quite interesting. It involves spins across the system. It also depends strongly on the concentration of the antiferromagnetic bonds. When the concentration is low, it is hard to find a spanning path that, when all spins on

one side are flipped, gives an excitation as low as $2J$. On the other hand if the concentration is high enough, we may expect that such a path can be easily found.

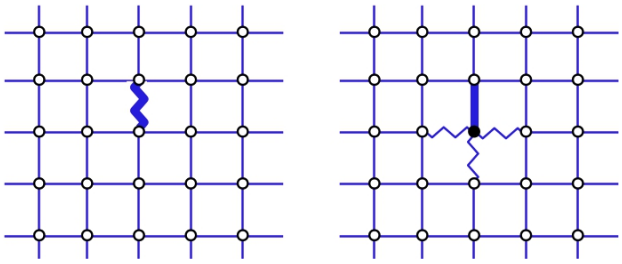

Figure 1.1: An example of a $4J$ excitation. In this system every bond is ferromagnetic (thin lines) except one bond in the middle which is antiferromagnetic (thick lines). White dots represent spin up and black dots represent spin down. Jagged lines represent unsatisfied bonds. On the left is a ground state configuration with one unsatisfied bond. On the right is a first excited state obtained by flipping a spin. The excited state has three unsatisfied bonds. The energy difference is thus $4J$.

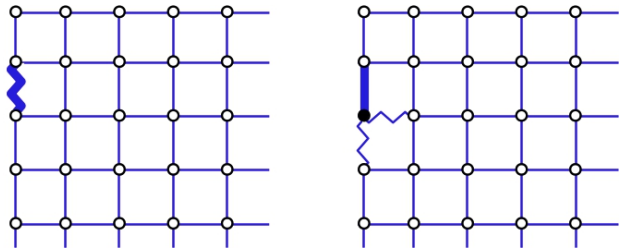

Figure 1.2: An example of a $2J$ excitation. A spin on the open boundary is flipped. The number of unsatisfied bonds is increased from one to two and the energy difference is $2J$.

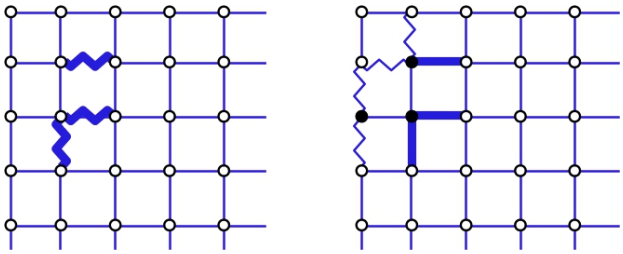

Figure 1.3: Another example of a $2J$ excitation. Three spins, with one spin on the boundary, are flipped. The number of unsatisfied bonds is increased from three to four, thus the energy difference is $2J$.

We believe that these spanning 2*J* excitations are the signature of the spin glass phase. It is interesting to see whether or not there is a sharp transition between two phases where the 2*J* excitations do not and do exist in the thermodynamic limit. It is even more interesting to see that whether this transition concentration coincides with the ferromagnetic-spin glass transition p_c or not.

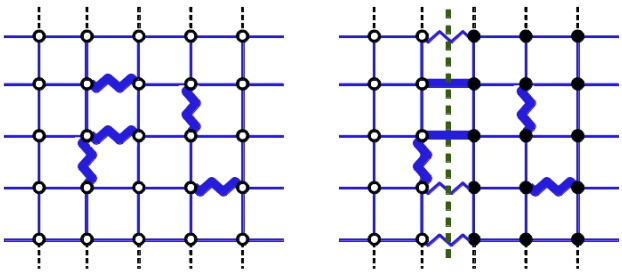

Figure 1.4: An example of spanning 2*J* excitation. On the left is a ground state configuration with five unsatisfied bonds. On the right is a first excited state obtained by flipping all spins on one side of the vertical broken line. The excited state has six unsatisfied bonds.

In principle, we may tackle this problem geometrically, although this is impractical for a large system. There is an exact algorithm to calculate the degeneracies of excited states [12]. It is practical to detect the spanning 2*J* excitations by measuring their degeneracies. However, in the open boundary system, there also exist local 2*J* excitations, as shown in figures 1.2 and 1.3. To focus on the spanning 2*J* excitations only, it is more convenient to work with an alternative boundary condition. We study the system with periodic boundary conditions in one direction, embedded in an infinite ferromagnetic nest in the second direction. We may have spanning 2*J* excitations if the linear dimension *L* in the direction of the periodic boundary is odd. These 2*J* excitations involve flipping all spins on one side of some closed path wrapping around the system. Figure 1.5 shows an example. Other closed paths can give excitations with energies equal to an odd multiple of 2*J*. There are no local (not spanning) 2*J* excitations in this system. Where the degeneracy of the 2*J* states is greater than zero, the spanning 2*J* excitations exist.

1.2.2 Distributions of Low-Lying States

Working with periodic-nested boundary conditions gives rise to the second issue of this thesis. It was shown [12] that if L is even, 2*J* excitations are not allowed. The closed paths give 4*J* excitations and the energy gap is 4*J*. For a system with full periodic boundary conditions (both directions), the spanning excitations need two closed paths and the energy gap is thus 4*J*. We now come to the situation that the size of the energy gap depends on the boundary conditions. This behaviour contradicts the requirement that physical quantities should be independent of boundary condition in the thermodynamic limit.

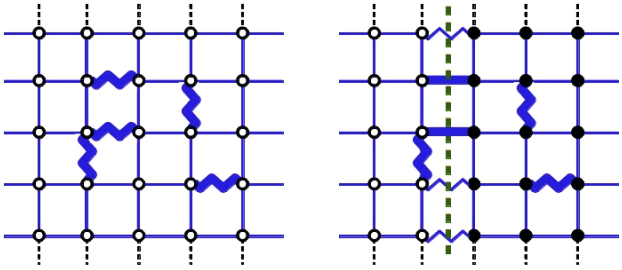

Figure 1.5: An example of a 2*J* excitation in the system with periodic boundary conditions in the *x*-direction and embedded in an infinite ferromagnetic nest in the *y*-direction. On the left is a ground state configuration with five unsatisfied bonds. On the right is a first excited state obtained by flipping all spins on one side of the vertical broken line. The excited state has six unsatisfied bonds.

We believe that these strange behaviours are closely related to the controversy of the low temperature thermal response, that is the specific heat, of the model. In the bimodal spin glass, since the energy levels are discrete, the partition function can be written as the sum over energy states of the Boltzmann weights

$$Z = 2 M_0 e^{-\frac{E_0}{kT}} \left(1 + \frac{M_1}{M_0} e^{-\frac{\Delta E_1}{kT}} + \frac{M_2}{M_0} e^{-\frac{\Delta E_2}{kT}} + \cdots \right) \tag{1.3}$$

where $\Delta E_i = E_i - E_0$. E_0 is the ground state energy and E_i is the energy of the *i*th excited state. M_0 is the ground state degeneracy and M_i is the degeneracy of the *i*th excited state. The factor 2 comes from global inversion. Using thermodynamic relations

$F = -kT \ln Z$, $S = -\frac{dF}{dT}$ and $E = F + TS$ together with the expansion $\ln(1+x) = x - \frac{x^2}{2} + \frac{x^3}{3} - \cdots$, we can write the specific heat as

$$\begin{aligned} c_v &= \frac{1}{L^2}\frac{dE}{dT} \\ &= \frac{1}{k(LT)^2}\left\{ \Delta E_1^2 \frac{M_1}{M_0} e^{-\frac{\Delta E_1}{kT}} + \Delta E_2^2 \left[\frac{M_2}{M_0} - \frac{1}{2}\left(\frac{M_1}{M_0}\right)^2 \right] e^{-\frac{\Delta E_2}{kT}} + \cdots \right\} \end{aligned} \tag{1.4}$$

Note that, since the above expansion of $\ln(1 + x)$ is valid only when $x < 1$, the relation for c_v is valid at low temperature only. If the temperature is low enough, we may naively expect that the first term dominates the series and the low temperature specific heat varies with the temperature as

$$c_v \sim \frac{E_g^2}{k(LT)^2}\frac{M_1}{M_0}\exp\left(-\frac{E_g}{kT}\right). \tag{1.5}$$

where $E_g = \Delta E_1$ is the energy gap. To get this relation we implicitly assume that the distribution of the ratio M_1/M_0 is sharp and we expect a definite value in the thermodynamic limit. However, it was found [12] that, for the canonical spin glass with even L, the distributions of the degeneracies of the low-lying states are broad and have fat tails, especially with increasing L. This means that we cannot assume the functional form of cv in equation 1.5. Even though there is an energy gap, saying that the ground states and first excited states dominate the low temperature physics may not be physically meaningful. For a finite system, we cannot lower the temperature beyond the point where ground states and first excited states start dominating the behaviour of the system.

Recently, there is a report [13] that the specific heat varies as a power law with the temperature. Since the calculations are performed for very large systems, this result is very reliable. The calculations are based on the assumption that the low temperature specific heat contains contributions from excitations having a range of energies. This idea seems to fit well with the discussion above that the low temperature physics may be not affected by the energy gap. The power law scaling of specific heat is similar to that of the Gaussian model, where the random interaction J_{ij}

is Gaussian distributed. It seems that in the thermodynamic limit the bimodal Ising spin glass model in two dimensions is “gapless” as in the Gaussian model.

For the second issue of this thesis, we want to show that broad distributions of the degeneracies of the low-lying states are also the characteristic of the spin glass phase. We believe that the broad distributions result from the existence of the spanning excitation paths. In the ferromagnetic phase, there are no spanning $2J$ paths in the thermodynamic limit. The energy gap should be $4J$, regardless of the boundary conditions. Since it is reasonable to expect that there are no spanning $4J$ paths either, the distributions of $4J$ states should be sharp. On the contrary, in the spin glass phase we can expect a lot of spanning paths, and the distributions of low-lying states should be broad.

To show this, we investigate the distributions of the low-lying energy states of the systems with the nested-periodic boundary condition, just above and below the critical concentration p_c. We believe that the results should reflect the characteristics of the other boundary conditions. We adapt the algorithm in [12,14] to calculate the degeneracies of the excited states for large numbers of disorder realisations. We then use a sophisticated algorithm to estimate the distributions of the degeneracies. The shape of distributions for both phases are then investigated. For the systems with odd L, the distributions of $2J$ states above and below p_c are compared. For the systems with even L, we investigate the distributions of $4J$ states. For comparison, we also investigate the distributions of $4J$ states for the system with odd L.

1.3 Objectives and Outline of the Thesis

In this thesis we propose to:

- Investigate the existence of spanning $2J$ excitations in the bimodal Ising spin glass model on a square lattice with periodic boundary conditions in one direction, embedded in an infinite ferromagnetic nest in the second direction, and odd L.

- Estimate the transition concentration that separates the two phases where the $2J$ excitations do not and do exist in the thermodynamic limit. Examine whether this coincides with the ferromagnetic-spin glass transition p_c or not.

- Investigate the distributions of low-lying states. Compare the shapes of the distributions above and below p_c. Examine whether a broad distribution is characteristic of the spin glass phase or not.

The detail of the our studies is given in the following chapters. After this introductory chapter, we review the related literature in chapter 2. The existence of $2J$ excitations, the mathematical formalism, and the computer algorithms used in our analyses are described in chapter 3. The results and discussion are then given in chapter 4. Chapter 5 summarises what we have done and introduces some interesting issues for further study.

CHAPTER II
LITERATURE REVIEW

The value of the energy gap of the bimodal Ising spin glass model is a long debated issue. This dates back more than two decades to the proposal of Wang and Swendsen [15], who performed the replica Monte Carlo simulations on system sizes $L \leq 32$ with periodic boundary conditions. They estimated that the specific heat at low temperature follows the exponential scaling

$$c_v \propto T^{-2} \exp\left(-\frac{A J}{k T}\right) \tag{2.1}$$

with $A \approx 2$. This result indicates that the energy gap is $2J$. This value is different from $4J$, which might be naively expected. They also performed transfer matrix calculations for the system with open boundary conditions. The results were reported to fit well with $A = 2$. They suggested that the $2J$ excitations are a nonlocal effect. They involve the rearrangement of a large number of spin orientations.

The idea of a $2J$ gap has afterwards been both challenged and supported. Saul and Kardar [16,17] performed exact calculations of the partition function for the system sizes $L \leq 36$ with periodic boundary conditions. They compared the entropy difference between the ground states and first excited states for the fully frustrated Ising model and the bimodal Ising spin glass, and suggested that both models should have a similar behaviour. Thus the specific heat of the bimodal Ising spin glass model should follow exponential scaling with $A = 4$. They also proposed an exponential scaling for the correlation length

$$\xi \propto \exp\left(\frac{n J}{k T}\right) \tag{2.2}$$

with $n \approx 2$. This behaviour of the correlation length supports the idea of $4J$ gap since it is consistent with the hyperscaling relation $A = 2n$.

Lukic et al. [18,19] calculated the low temperature specific heat for system

sizes $L \leq 50$ with periodic boundary conditions, using exact calculations for partition functions. They proposed that when L is large the low temperature specific heat will follow exponential scaling with $A = 2$. They also suggested the noncommutativity of the zero-temperature and thermodynamic limit. To study the low temperature properties of this model, the thermodynamic limit has to be taken at some finite temperatures first, following by the zero-temperature limit.

Katzgraber and Lee [20] performed simulations on the system sizes $L \leq 128$ with periodic boundary conditions, using combined the parallel tempering Monte Carlo method and rejection-free cluster algorithm. They proposed that the correlation length follows exponential scaling with $n = 2$, in agreement with [16,17]. Using the hyperscaling relation, they suggested that the energy gap should be $4J$.

Wang [21] performed the Monte Carlo simulations using the worm algorithm on the system sizes $L \leq 128$ with open and periodic boundary conditions. He found that for the systems with an open boundary, the specific heat follows the exponential scaling with $A \approx 2$. For the system with full periodic boundary conditions, there is a crossover temperature where the specific heat bends to follow exponential scaling with $A = 4$. The crossover temperature becomes smaller with increasing L. This suggests that the $4J$ excitation is a finite size effect exhibited with finite systems when the temperature is too low.

Katzgraber et al. [22] performed an alternate analysis of the data presented in [20]. They found that the correlation length scales exponentially with $n = 1$, in contrast to their previous calculations. They also performed direct calculations of the specific heat on the system sizes $L \leq 64$. The results suggests that for large enough system sizes L and low enough T, the specific heat follows exponential scaling with $A = 2$, which is consistent with the hyperscaling relation $A = 2n$. They also emphasized that to understand the low temperature properties of this model, the limit of $L \rightarrow \infty$ has to be taken before extrapolating to $T = 0$.

Recently, Atisattapong and Poulter [12] performed exact calculations of the degeneracies of the low-lying states on system sizes $L \leq 96$. Their algorithm is based on the Pfaffian formalism and degenerate state perturbation theory [14]. They used periodic boundary conditions in one direction, embedded in an infinite ferromagnetic

nest in the second direction, and even L. With these boundary conditions, $2J$ excitations are not allowed, and the first excitation has to be $4J$. The distributions of the ratio of first excited states and ground states M_1/M_0 were calculated from a large number of disorder realisations (up to 10^5). They found that the peaks of the distributions of this ratio per spin scale as L. Using exponential scaling of the correlation length with $n = 2$ [20], they suggested that the "effective" energy gap of the system should be $2J$, in apparent violation of hyperscaling.

Up to this point, it is not clear what is the energy gap of the system. If we consider an infinite system, the energy gap can be naively expected to be $4J$. However, as discussed in the previous chapter, the $2J$ excitations can occur in finite systems with certain boundary conditions. One may interpret this as a boundary effect which should vanish in the thermodynamic limit. Anyway, it was pointed out by Binder and Young [3] that the boundary effect is important in this complicated system, even in the limit $L \rightarrow \infty$. Mimicking the infinite system with periodic boundary conditions may be not appropriate for this model.

There are also the issues on the distributions of the low-lying states. The exponential scaling of specific heat comes from the assumption that the energy levels are discrete. It also needs the implicit assumption that the degeneracies of the low-lying states have a definite value in the thermodynamic limit. Thus, when the temperature is low enough, the ground states and first excited states should dominate the behaviour of the specific heat. Sharpness of the distribution of degeneracy implies that this quantity has the self-averaging property, that is, the relative variance of the distribution approaches zero in the thermodynamic limit [3]. This property is expected for experimental observable quantities. Dayal et al. [23], studied the performance of flat-histogram methods and found that, for the bimodal Ising spin glass, the ratios M_1/M_0 are fat-tailed Fréchet distributed [24]. Atisattapong and Poulter [12] confirmed these results. They also found that the distributions are collapsing in height with increasing L. A sharp distribution of M_1/M_0 is unlikely in the thermodynamic limit, and we may need to reconsider the exponential scaling of the specific heat.

Recently, there has been an alternative idea that at finite but low temperatures in the thermodynamic limit, the bimodal Ising spin glass model falls into

the same universality class as the gapless, Gaussian model. Within this scenario the low temperature correlation length and specific heat will vary with temperature as a power law

$$\xi \propto T^{-\nu} \quad \text{and} \quad c_v \propto T^{-\alpha} \tag{2.3}$$

Jörg et al. [25] combined Monte Carlo simulations and exact calculations of partition functions to calculate the correlation length and specific heat for system sizes $L \leq 80$. The results suggested that both quantities should follow a power law. They estimated the value of $\nu \approx 3.5$. The value of α was indirectly estimated through the hyperscaling relation [26] as $\alpha = -2\nu \approx -7$.

Later Katzgraber et al. [27] performed Monte Carlo simulations on system sizes larger than that used in [25] ($L \leq 128$). They directly calculated the low temperature specific heat and found that it varies with the temperature as a power law with $\alpha \approx -4.2$.

Most recently, Thomas et al. [13] performed exact calculations of partition functions on very large systems sizes ($L \leq 512$). They proposed that at very low temperature the specific heat varies as a power law with $\alpha = -3$, which is greater than -4.2 or -7. It seems that, although the power law scaling is very plausible, it is still not clear what the value of α is exactly. Also note that, for the case of Gaussian disorder, the direct calculations of Cheung and McMillan [28] and Houdayer and Hartmann [29] report that the low temperature specific heat is linear with $\alpha = -1.0$. Universality is hard to prove.

A related issue is the study of domain wall defects [30–35]. The domain wall is a spanning path with its weight equal to the difference of ground state energies when we change the boundary condition from periodic to antiperiodic. The weight of a path is defined as the energy difference when all bonds crossed by the path change their signs while the spins orientations are fixed. In the ferromagnetic phase, introducing domain walls into the system will give rise to a ground state energy proportional to the linear dimension L. In the spin glass phase, the domain wall can either increase or decrease the energy. From these different behaviours of the domain wall defect, we may analyse the stability of the spin glass phase [10,36].

Introducing the domain wall also changes the entropy of the system. It was suggested that the deviation of entropy difference is scaled as [37]

$$\{[\delta S^2]-[\delta S]^2\}^{1/2}\sim L^{\theta} \tag{2.4}$$

where δS is the difference of ground state entropy when we change the boundary condition from periodic to anti-periodic. The square bracket $[\cdot\ \cdot\ \cdot\ ]$ represents the disorder average. The fractal dimension df of a domain wall is related to the exponent θ as $d_f = 2\theta$ [37,38]. This relation gives a way to measure the fractal dimension of domain wall defects.

Although it is stated that a domain wall has a multifractal structure, Thomas et al. [13] proposed that $\theta = 0.5$. This value agrees well with Saul and Kardar [17] who stated that the domain wall defects are non-fractal objects. Lukic et al. [39] performed exact calculations of partition functions for system sizes $L \leq 50$ and obtained the value of $d_f = 1.03(2)$. They expected that the exact value of d_f should be 1.

Other works report that $d_f > 1$. Romá [40] used the matching method [5] to directly obtain the domain wall fractal dimension for system sizes $L \leq 100$. They found that $d_f = 1.30(2)$. Weigel and Johnston [41] used the same method for system sizes $L \leq 256$ and found $d_f = 1.238(11)$. Aromsawa and Poulter [42] performed exact calculations using the Pfaffian method and degenerate state perturbation theory [14] for system sizes $L \leq 256$. They obtained the value of $d_f = 1.30(3)$ for $L \geq 96$. Melchert and Hartmann [43] also used the matching method [5] to directly obtain the domain wall fractal dimension for system sizes $L \leq 256$. They proposed that the fractal dimension should lie between $1.095(2) \leq d_f \leq 1.395(3)$. Note that they also found that there are a lot of domain walls with $2J$ weight. This supports our expectation that the spanning $2J$ excitations are possible in the spin glass phase.

It is not clear what the value of df is. This issue is also related to the problem of the value of α. Based on the droplet theory [37,38], Thomas et al. [13] proposed that at very low temperature T the specific heat varies as

$$c_v \propto T^{(2/\theta)-1} \tag{2.5}$$

which means $\alpha = 1 - 2/\theta$. The value $\theta = 0.5$(or $d_f = 1$) gives $\alpha = -3$. If $d_f > 1$,then

$\theta > 0.5$ and, according to equation 2.5, this gives α greater than -3.0. It seems unlikely that droplet theory can predict a value in agreement with $\alpha = -4.2$ or $\alpha = -7$.

We can see that the issues of the energies and distributions of low-lying states are still controversial. The energy gap seems to depend strongly on the boundary conditions, which is against the requirement of a physical quantity. Also, it is still not clear how the behaviour of the system with discrete energy levels approaches that of the continuous one in the thermodynamic limit. The most reliable work now seems to be [13], since they work with very large system sizes (up to $L = 512$). Nevertheless their power law scaling of specific heat is valid in a very narrow temperature range. The exponent α does not agree with other works, as discussed above.

However, one thing that is quite clear now is that the low-temperature specific heat contains contributions from excitations having a range of energy. Katzgraber et al. [27] suggested that we cannot lower the temperature beyond a certain point T_ξ where the correlation length $\xi(T) \sim L$. They found that above T_ξ the effect of the energy gap can be neglected. The specific heat is involved with a range of energy states, and the power law scaling is exhibited.

Thomas et al. [13] explained this using the droplet theory [37, 38]. The idea is that reversing all spins in a compact cluster (droplet) with respect to a ground state provides an excitation. Typical droplet excitations dominate the thermodynamic behaviour. It is assumed that the scaling behaviour of the energy and entropy of a droplet are similar to those of domain wall defects [13]. Thus, we may have large droplets with *small energies* [43] but *very large entropies* (since $\theta > 0$). This leads us to assume that, due to their large entropies, a range of excited states can be occupied even at very low temperature.

To our knowledge, none of the works mentioned above (except [12] and [23]) have studied the sizes and distributions of low-lying energy states directly. Those two exceptions used boundary conditions that do not allow $2J$ excitations. Further studies of the $2J$ states and their distributions would thus be very interesting.

CHAPTER III
FORMALISM AND METHOD

3.1 Boundary Conditions and the Energy Gap

As discussed in the first chapter, it seems that the energy gap of the bimodal Ising spin glass model in two dimensions depends strongly on the boundary conditions. In this section we discuss this issue in more detail.

3.1.1 Infinite Systems

Let us start with the Ising model with pure ferromagnetic interactions on an infinite lattice. In the ground state, all spins are aligned in the same direction, and all bonds are satisfied. The first excited states can be achieved by flipping a single spin, as shown in figure 3.1. The energy gap is $8J$. Flipping this spin also changes the status of the bonds connected to that spin. We can see that four bonds connected to the flipped spin change their status from satisfied to unsatisfied. Thus it is equivalent to say that we can excite the system by changing the status of some bonds.

We may represent an excitation by a *path* crossing the bonds that change their status. The dashed path in figure 3.1 is an example of a path corresponding to a single spin flipping. Since each bond cannot change its status independently, the excitation paths in the infinite system have to be closed. In the ferromagnetic system, reversing all spins inside a closed path gives us an excited state.

Let us define the *length* of a path by the number of bonds crossed by the path. In the infinite system, the length of a *closed* path l_c is

$$l_c = 2(n+1), \quad n = 1,2, \ldots \tag{3.1}$$

We can see that l_c is an even number. The minimum value of l_c is 4.

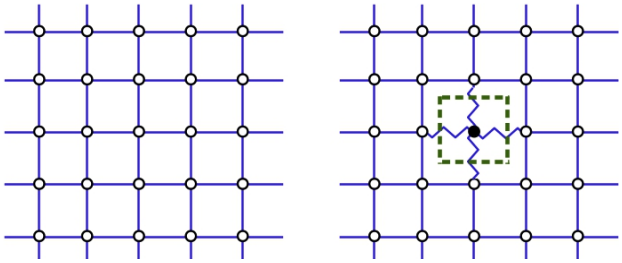

Figure 3.1: An example of an $8J$ excitation. In this system every bond is ferromagnetic. On the left all spins are up and the system is in a ground state. On the right is a first excited state obtained by flipping a spin. Four bonds connected to the flipped spin change their status from satisfied to unsatisfied. The length of the dashed path is 4 and the weight is $8J$.

The weight ω of a path is defined as

$$\omega = 2J \sum_i \delta_i , \tag{3.2}$$

where the summation is over all bonds crossed by the path, and

$$\begin{aligned} \delta_i &= 1 \quad \text{if bond } i \text{ changes from satisfied to unsatisfied} \\ &= -1 \quad \text{otherwise.} \end{aligned} \tag{3.3}$$

The weight of a path is equal to the energy introduced into the system by reversing all spins enclosed by the path.

In the ferromagnetic system, the smallest excitations are given by the shortest path. Since the smallest value of l_c is 4, the weight of this path is $8J$, which is the energy of first excited states.

Now, let us introduce antiferromagnetic defects into the system. We can see that, in the ground states, some bonds are not satisfied. When the concentration p of the antiferromagnetic bonds is low, the unsatisfied bonds are widely separated. As p increases, the unsatisfied bonds come closer and form clusters. Figure 3.2 shows some examples of isolated and clustered unsatisfied bonds.

The excitations can be achieved by flipping spins inside the closed paths, as in the the pure ferromagnetic system. However, some closed paths may give another

ground state. The shortest paths do not necessary have the smallest weight. Since the lengths of the closed paths l_c are even, if there are n bonds with $\delta_i = 1$, there will be $m = l_c - n$ bonds with $\delta_i = -1$. The weights of the paths are $\omega = 2J(n - m)$. Since $n + m = l_c$ is always even, $n - m$ is zero or even. The weights of the paths are either zero or an even multiple of $2J$. If the weight is zero, flipping the spins inside the closed path just gives us another ground state. The energy gap corresponds to the paths with smallest positive weight and is equal to $4J$. Some examples of $4J$ excitations are shown in figure 3.3.

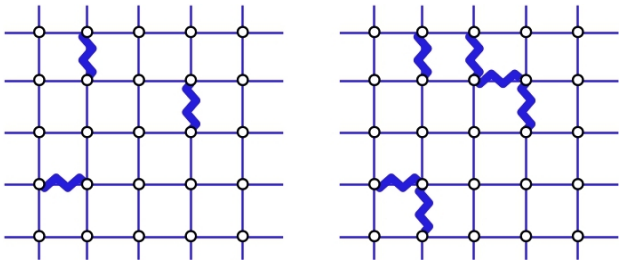

Figure 3.2: Examples of ground states with isolated (left) and clustered (right) unsatisfied bonds.

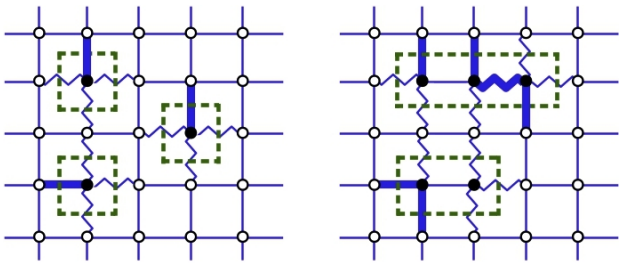

Figure 3.3: Examples of $4J$ excitation paths from the ground states in figure 3.2.

3.1.2 Systems with Open Boundary

We now move to finite systems with an open boundary. An excitation involving spins that are not on the boundary can be presented by a closed path, as in the infinite system. However, if some spins are on the boundary, the corresponding paths are open. Reversing the spins on one side of this path gives us either excited state or another ground state.

The length of the open paths can be either even or odd. For an open path, if

there are n bonds with $\delta_i = 1$and m bonds with $\delta_i = -1$, the length l_o and weight ω of this path are $n + m$ and $2J(n - m)$ respectively. With even l_o, the weight is either zero or an even multiple of $2J$. This is similar to the cases of the closed paths. With odd l_o, we can see that $n \neq m$. If n is even, m is odd, and vice versa. The difference $n - m$ is always an odd number. The weight is an odd multiple of $2J$. Thus, the energy gap is the smallest positive weight and is equal to $2J$.

When the concentration p is low, the unsatisfied bonds are widely separated, and only few of them may be on the boundary. The $2J$ excitations correspond to short open paths. An example is shown in figure 3.4. As p increases, the unsatisfied bonds come closer to the boundaries, and we can have longer paths with $2J$ weight. Figure 3.5 gives an example.

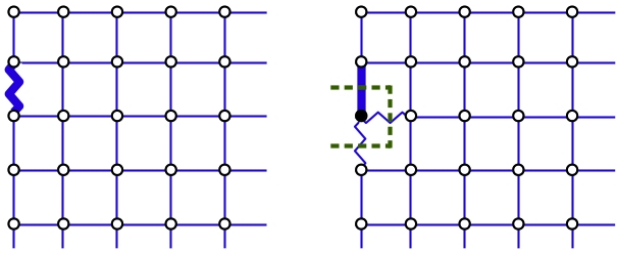

Figure 3.4: An example of an excitation involved with an open boundary. In the ground state one bond on the boundary is unsatisfied. Flipping a spin on the left side of the open path gives the energy $2J$ to the system.

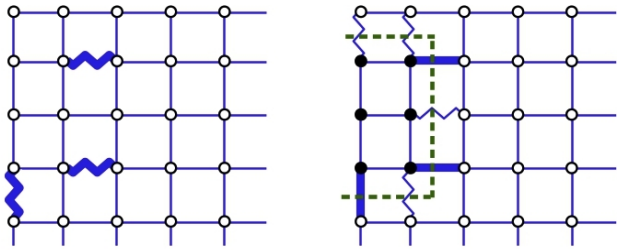

Figure 3.5: Another example of an excitation involved with an open boundary. Once the unsatisfied bonds come closer to the boundary, it is possible to have longer paths with $2J$ weight.

We are interested in the case when p is large enough that there exist the open paths with $2J$ weight that span across the system. Figure 3.6 shows an example.

Their existence depends strongly on the amount of unsatisfied bonds. We must have the path with length scale L and $n - m = 1$. The system needs enough "frustration" for spanning $2J$ paths to exist. We believe that this is the signature of the spin glass phase. We expect that there is a sharp transition between two phases where the $2J$ excitations do not and do exist in the thermodynamic limit, and this transition coincides with the ferromagnetic-spin glass transition concentration p_c.

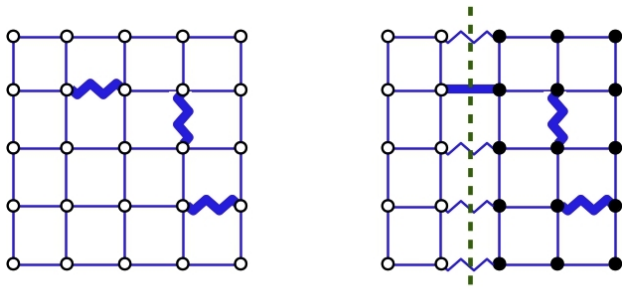

Figure 3.6: An example of a spanning path with $2J$ weight. Flipping all spins on one side of the path excites the ground state with the energy $2J$.

In principle, the spanning $2J$ paths can be detected geometrically. However, the huge degeneracy of the $2J$ states makes it impractical to do so. We indirectly investigate the $2J$ spanning paths by calculating the degeneracies M_1 of the $2J$ states. The exact algorithm [12] used in the calculations is explained later in this chapter. We also, of course, have the non-spanning $2J$ paths counted in M_1. To focus on the spanning $2J$ paths, it is more convenient to work with an alternative boundary condition where only the spanning $2J$ paths can exist. These kinds of boundary conditions are discussed in the next section.

3.1.3 Systems with Periodic Boundary Conditions in One Direction, and Infinite Ferromagnetic Nest in the Second Direction

Consider system with periodic boundary conditions in one direction and embedded in an infinite nest in the second direction, as an example in figure 3.7. In the nest all bonds are ferromagnetic. Since there are no open boundaries, any excitations can be represented by closed paths. However, there are two kinds of closed paths. The

first kind are the closed paths that are not wrapped around the system. The length of these paths are always even and their weights are either zero or an even multiple of 2*J*, as discussed previously.

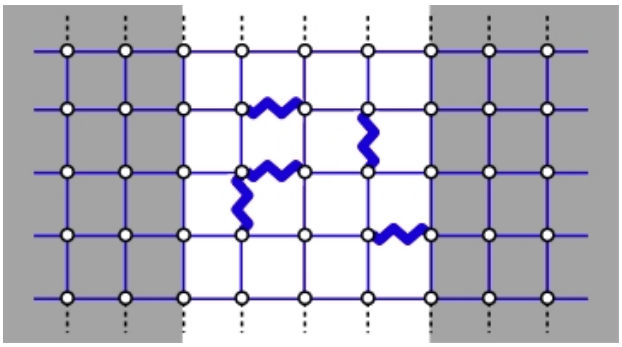

Figure 3.7: A 5 × 5 lattice with periodic boundary conditions in the *y*-direction (dashed lines), and embedded in an infinite nest (grey area) in the *x*-direction. All bonds in the nest (including the bonds on the boundaries of the nest) are ferromagnetic.

The second kind are the wrapped paths that wrap around the system. We can see that the length of a wrapped path l_w is

$$l_w = L_{pb} + 2n, \quad n = 1, 2, \ldots \tag{3.4}$$

Here L_{pb} is the linear dimension of the system in the direction of periodic boundaries. We can excite the system by flipping all spins on one side of the wrapped paths. The energy gained is equal to the weight of the path.

If L_{pb} is odd, l_w is odd, and vice versa. In the systems with odd L_{pb}, the weights of wrapped paths are an odd multiple of 2*J*. When the concentration *p* is large enough, we may have $n - m = 1$ on the wrapped paths, and the energy gap is thus 2*J*. An example is shown in figure 3.8.

These wrapped 2*J* paths can be used to mimic the situation of spanning 2*J* paths in the open system. However, the advantage of studying the wrapped 2*J* paths is that we can detect them by measuring M_1. Since the 2*J* excitations come from the wrapped paths only, if $M_1 > 0$, then the wrapped 2*J* paths exist. In the ferromagnetic phase M_1 is zero since there is not enough frustration in the system, while in spin glass

phase $M_1 > 0$. There must be a transition concentration when M_1 changes from zero to a finite value, and this transition concentration should coincide with the ferromagnetic-spin glass transition concentration p_c.

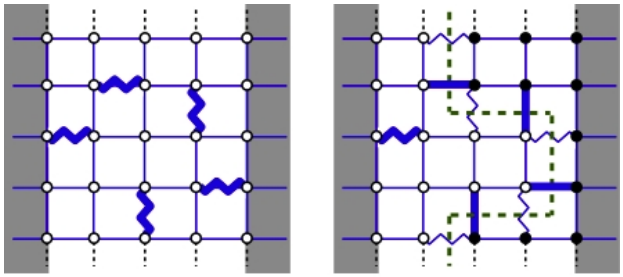

Figure 3.8: An example of a wrapped path with $2J$ weight. The length $l_w = 9$, $n = 5$, and $m = 4$. Flipping all spins on the right side of the dashed path excites the ground state with energy $2J$.

If L_{pb} is even, the weights of wrapped paths are either zero or an even multiple of $2J$. This mean that $2J$ excitations are not allowed. The energy gap is thus $4J$. These $4J$ excitations can come from both kinds of closed loops. So it is impossible to detect the wrapped $4J$ paths by measuring the degeneracy of the $4J$ states. Therefore the periodic-nested boundary conditions with odd L_{pb} are the most suitable devices to study the spanning $2J$ excitations in the bimodal Ising spin glass model.

3.1.4 Systems with Full Periodic Boundary Conditions

We finish this section by considering the systems with periodic boundary conditions in both directions. Since there are no open boundaries, the excitation paths are always closed. For the unwrapped paths, the excitation energies are an even multiple of $2J$. We can also excite the system with wrapped paths. However, due to the boundary conditions, we can not flip all spins on one side of a wrapped path. An even number of wrapped paths is needed to excite the systems. All spins in between two wrapped paths can be flipped which gives an energy equal to the total weight of those two paths. Since the numbers of wrapped paths are even, the total lengths are also always even. The total weights are either zero or an even multiple of $2J$. The energy gap is the smallest, positive weight of either the closed or wrapped paths, this is $4J$.

To summarise the section, we have seen that the size of the energy gaps of finite systems depends strongly on the boundary conditions. In the systems with open boundary the energy gaps are obviously $2J$ while in the systems with full periodic boundary conditions the energy gaps are $4J$. In the systems with periodic-nested boundary conditions the energy gaps also depend on the concentration of negative bonds and the sizes of L_{pb}. These do not seem to fit the requirement that the physical quantities should not depend on the boundary conditions. However, it is discussed later that the size of the energy gap should not have much effect much on the physical quantities. A proper description of the model should involve a large number (if not all) of energy states. The measurement of any physical quantities should be the same no matter what the energy gap is.

Although the size of the energy gap depends on the boundary conditions, there is a common feature of the low-lying excitations. When the concentration of negative bonds is large enough, there exist spanning or wrapped paths with the smallest possible weight. We believe that the existence of these paths is the signature of the spin glass phase since it depends on the amount of frustration in the system. Once there is enough frustration, we can have the smallest excitations that involve many spins across the system.

Understanding these kinds of paths with one boundary condition should shed light on the others. As discussed above, the systems with periodic-nested boundary conditions and odd L_{pb} are good devices. Since there are no local $2J$ paths, we can detect the wrapped paths by measuring the degeneracies of $2J$ states. In the next section the exact algorithms use to measure the degeneracies are discussed.

3.2 The Pfaffian Method and Degenerate State Perturbation Theory

This section is intended to be the “recipe” of how to calculate the degeneracy of excited states, including 2J states. Detail derivations can be found in [12,14,44–46].

The algorithms are based on the formalism proposed by Green and Hurst

[44]. For a planar Ising model with $N = L \times L$ lattice sites, the partition function can be written as

$$Z = 2^N \left[\prod_{\langle ij \rangle} \cosh\left(\frac{J_{ij}}{kT} \right) \right] (\det D)^{1/2}. \tag{3.5}$$

This formula is valid for any distribution of disorder. The product is over all nearest-neighbour bonds J_{ij} on an N site lattice. The matrix D is a $4N \times 4N$ skew-symmetric matrix associated with the four-node decomposition of the original lattice, as shown in figure 3.9. It comprises constant 4×4 diagonal blocks which represent the "intrasite connections" between these four nodes, as shown in equation 3.6,

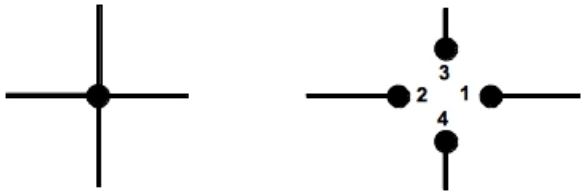

Figure 3.9: Four-node decomposition of the original lattice.

$$D_{\text{intrasite}} = \begin{bmatrix} 0 & -1 & 1 & 1 \\ 1 & 0 & -1 & 1 \\ -1 & 1 & 0 & -1 \\ -1 & -1 & 1 & 0 \end{bmatrix}. \tag{3.6}$$

It also contains the "inter-connection" between nearest neighbour sites

$$\begin{aligned} D_{1,2} &= -t_{ij}, \quad D_{2,1} = t_{ij} \\ D_{3,4} &= -t_{ij}, \quad D_{4,3} = t_{ij} \end{aligned} \tag{3.7}$$

where $t_{ij} = \tanh(J_{ij}/kT)$. The graphical representations are shown in figure 3.10. Since D is skew-symmetric, the factor $(\det D)^{1/2}$ is precisely the Pfaffian.

It is more convenient to change the representation of D to bond basis. The bond basis is defined as the following linear combinations of the node basis

$$|\pm\rangle = \frac{1}{\sqrt{2}} \left(|\alpha\rangle \pm \zeta_{ij} |\beta\rangle \right), \tag{3.8}$$

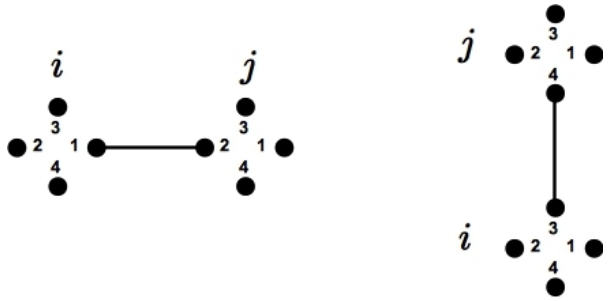

Figure 3.10: Inter-connection between nearest neighbour sites.

where $|\alpha\rangle$ and $|\beta\rangle$ are in the original node basis and ζ_{ij} is the sign of bond J_{ij}. This transformation is graphically shown in figure 3.11. The advantage of using the bond basis is that it is plaquette-oriented. For a square lattice, the plaquette is an elementary square surrounded with four bonds. Each plaquette has four bond-nodes inside and four others across the bonds, as shown in figure 3.12. Any matrix operations can be graphically represented as either the intra-connection between nodes inside a plaquette or the inter-connection between nodes in different plaquettes. This graphical interpretation is very helpful in the coding process.

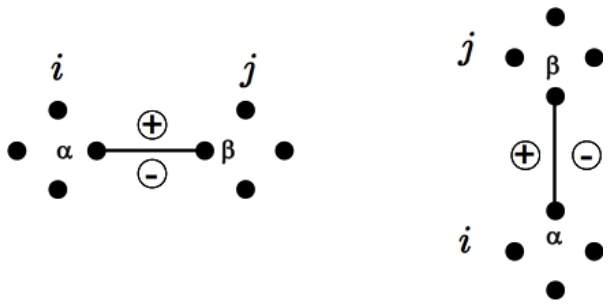

Figure 3.11: Transformation to bond basis.

A plaquette is said to be frustrated if there are odd numbers of negative bonds around it. Introducing a single negative bond to the system gives a pair of frustrated plaquettes, as shown in figure 3.13. We can see that not every bond around the frustrated plaquette can be satisfied, particularly in the ground state. This "frustration" is a key feature of the spin glass. Increasing the number of negative bonds or "defects" will increase the number of frustrated plaquettes, and thus the number of unsatisfied bonds. Once the defect concentration is large enough, the ferromagnetism will be destroyed, and system will be in the spin glass phase.

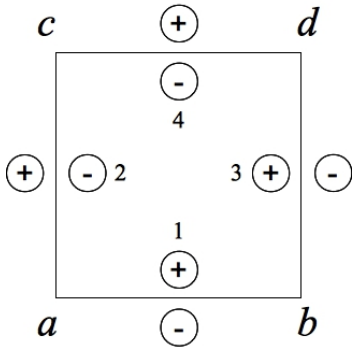

Figure 3.12: An example of a plaquette with four bond-nodes inside and four others across the bonds. The numbers are the labels of the bond basis associated with the plaquette, while the lattice sites are labeled by the letters.

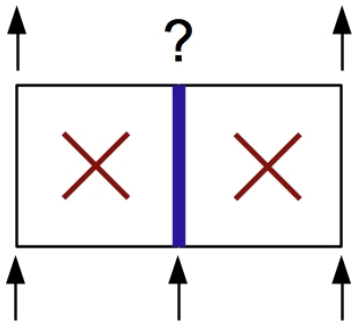

Figure 3.13: A pair of frustrated plaquettes with a single negative bond in the middle. In the ground state this middle bond is unsatisfied.

With a single negative bond, it was shown [45] that, at zero temperature, the matrix D will have a pair of defect states with zero eigenvalues. The defect eigenvectors can be written in the form

$$|d\rangle=\frac{1}{2}(|1\rangle+|2\rangle+\zeta_{ab}|3\rangle+\zeta_{ac}|4\rangle), \tag{3.9}$$

where we use the labels in figure 3.12. We can see that the eigenvectors are localised in the frustrated plaquettes. At low temperature the defect eigenvalues approach zero as

$$\epsilon = \pm\frac{1}{2}\exp\left(-\frac{2J}{kT}\right). \tag{3.10}$$

With an arbitrary number of negative bonds, the number of frustrated plaquettes is always even. It was shown [14] that, in general, at zero temperature, there are defect eigenstates with zero eigenvalues. The number of defect eigenstates is equal to the number of frustrated plaquettes. Each defect eigenvector is localised in the frustrated plaquettes with the form as in equation 3.12. The defect eigenvalues approach zero as

$$\epsilon_d = \pm\frac{1}{2}X_d\exp\left(-\frac{2Jr_d}{kT}\right), \tag{3.11}$$

where r_d is an integer, and X_d is a real number. Both r_d and X_d are independent of temperature and depend on the distribution of frustrated plaquettes.

Note that, in the actual calculation, after we randomly place the negative bonds to the system, we perform local transformations [47] so that the negative bonds are vertical only. This transformations do not change the distribution of frustrated plaquettes, and thus do not change the defect eigenvalues too. This reduces the complexity of the problem, and the logical test time in the calculation. The defect eigenvectors can be rewritten in the form

$$|d\rangle = \frac{1}{2}(|1\rangle + |2\rangle + |3\rangle + \zeta_{ac}|4\rangle), \tag{3.12}$$

The ground state energy and entropy are shifted from that of the pure ferromagnetic system by

$$\Delta E = 2J\sum_{d}^{+} r_d, \tag{3.13}$$

$$\Delta S = k\sum_{d}^{+} \ln X_d. \tag{3.14}$$

From the last equation, it is equivalent to say that the ground state degeneracy is

$$M_0 = \prod_{d}^{+} X_{d.} \tag{3.15}$$

Note that the above summations and product are over all eigenstates with positive eigenvalues.

Although the ground states are not our main concern in this thesis, the information obtained from ground states calculations are needed to get the properties of the excited states properties. According to equations 3.13 and 3.14, the parameters r_d and X_d are needed to obtain the ground state energy and entropy. This information can be achieved by solving the eigenvalue equation of D at low temperature. Since the zero temperature defect eigenstates are degenerate, we use degenerate state perturbation theory [14] to separate the low temperature eigenvalues. At finite temperature the matrix D can be written as

$$D = D_0 + \delta D_1 , \tag{3.16}$$

where D_0 is the matrix D at $T = 0$, and $\delta = 1 - t = 1 - \tanh(J/kT)$. From this definition, D_1 has only non-zero elements connecting 2 bond-nodes across bonds,

$$D_1(+,-) = -D_1(-,+) = -1 . \tag{3.17}$$

Note that at low temperature

$$\delta \simeq 2\exp\left(-\frac{2J}{kT}\right) \tag{3.18}$$

The eigenvalue equation is

$$D|\Psi\rangle = \lambda|\Psi\rangle \tag{3.19}$$

where the eigenvalue λ can be written as the expansion

$$\lambda = \lambda_0 + \lambda_1\delta + \lambda_2\delta^2 + \cdots . \tag{3.20}$$

Here $\lambda_0 = 0$ is the zero temperature eigenvalue and λ_r is the r^{th} order correction term. We use δ as a small parameter for a perturbation expansion. Comparing with equation 3.11 we can see that the integer r_d is indeed the order of the perturbation correction. The parameter X_d of the i^{th} eigenvalue of order r can also be determined from the relation $(X_d)_r^i = 2\lambda_r^i$.

For the first order perturbation correction, the eigenvalue λ_1^i can be

obtained by solving the eigenvalue equation [14]

$$D_1|1,i\rangle=\lambda_1^i|1,i\rangle. \tag{3.21}$$

For second order we need to know the continuum Green's function G_c, which correspond to the ground state eigenvector $|c\rangle$ with non-zero eigenvalue ϵ_c as [14,46]

$$G_c=\sum_c|c\rangle\frac{1}{\epsilon_c}\langle c|, \tag{3.22}$$

where

$$\sum_c|c\rangle\langle c|+\sum_d|d\rangle\langle d|+1. \tag{3.23}$$

However, it is more convenient to work with the alternative Green's function g_c, which is defined according to

$$G_c=(1-P)\,g_c(1-P) \tag{3.24}$$

where

$$P=\sum_d|d\rangle\langle d|. \tag{3.25}$$

We can write $g_c = g_{c1} + g_{c2}$ [46], where g_{c1} has elements connecting the bond-nodes within a plaquette while g_{c2} has elements connecting bond-nodes across a bond, that is, $g_{c2}(+,-) = g_{c2}(-,+) = 1$. We may write g_{c1} as a 4×4 block diagonal matrix corresponding to the basis of four bond-nodes in a plaquette. For an unfrustrated plaquette this block matrix can be written as

$$g_{c1}^u=\begin{bmatrix}0 & 1 & -1 & \zeta_{ac}\\ -1 & 0 & -1 & \zeta_{ac}\\ 1 & 1 & 0 & \zeta_{ac}\\ -\zeta_{ac} & -\zeta_{ac} & -\zeta_{ac} & 0\end{bmatrix}. \tag{3.26}$$

Here we use the same labels as in figure 3.12. For a frustrated plaquette we have

$$g_{c1}^{f}=\begin{bmatrix} 0 & 1 & -1 & 0 \\ -1 & 0 & 0 & \zeta_{ac} \\ 1 & 0 & 0 & -\zeta_{ac} \\ 0 & -\zeta_{ac} & \zeta_{ac} & 0 \end{bmatrix}. \tag{3.27}$$

Once g_{c1} is calculated, the eigenvalue λ_2^i can be obtained by solving

$$D_2|2,i\rangle=\lambda_2^i|2,i\rangle. \tag{3.28}$$

where

$$D_2=D_1 g_{c1} D_1. \tag{3.29}$$

For higher orders $r > 2$, the eigenvalue λ_r^i can be obtained by solving [14]

$$D_r|r,i\rangle=\lambda_r^i|r,i\rangle. \tag{3.30}$$

Here D_r can be calculated recursively from the relation

$$D_r=D_{r-1}(1+G_{r-2}D_{r-2})\cdots(1+G_1 D_1) g_{c1} D_1, \tag{3.31}$$

where G_j is the Green's function for state j whose the degeneracy has already been lifted,

$$G_j=\sum_i |j,i\rangle\frac{1}{\lambda_j^i}\langle j,i|. \tag{3.32}$$

When all the D_r and G_r, and also g_{c1}, are obtained, we can move forward to the excited states. At arbitrary low temperature, the internal energy can be expanded as a series of exponential functions (see section 1.2.2)

$$E=E_0+\sum_{m=1}^{\infty} U_m \exp\left(-\frac{2mJ}{kT}\right). \tag{3.33}$$

Here E_0 is the ground state energy

$$E_0=-2NJ+\Delta E, \tag{3.34}$$

where ΔE can be obtained from equation 3.13. The cumulant U_m can be expressed in terms of the degeneracies M_i, for example

$$
\begin{aligned}
U_1 &= 2J\left(\frac{M_1}{M_0}\right) \\
U_2 &= 4J\left[\frac{M_2}{M_0} - \frac{1}{2}\left(\frac{M_1}{M_0}\right)^2\right] \\
U_3 &= 6J\left[\frac{M_3}{M_0} - \frac{M_1}{M_0}\frac{M_2}{M_0} + \frac{1}{3}\left(\frac{M_1}{M_0}\right)^3\right].
\end{aligned}
\tag{3.35}
$$

When the values of U_m are known, the degeneracies M_i can be calculated recursively.

We calculate U_m using the method described in [12]. The value of U_m can be obtained from the trace of a matrix

$$U_m = -2J \operatorname{Tr} R^m, \tag{3.36}$$

where the matrix R is obtained from

$$R = D_1 g_{c1}(1 + D_1 G_1)(1 + D_2 G_2)\cdots(1 + D_{r_{\max}} G_{r_{\max}}) \tag{3.37}$$

Here $r_{\max}$ is the maximum order of perturbation theory needed to identify all ground states eigenvalue. We can see that once the ground state calculations are finished, we can immediately calculate R. The cumulants U_m, and thus the degeneracies M_i, can finally be obtained.

3.3 Data Analysis

3.3.1 Transition Concentration

As the first issue of this thesis, we hypothesise that, in the thermodynamic limit, there is a sharp transition concentration where the probability of getting a $2J$ excitation changes from 0 to 1. In a finite system, finite size effects will smear out this sharp transition. However, we can estimate the p_c from the behavior of the system when L is increasing. Let us denote P_1 as the probability of getting $2J$ states. In the ferromagnetic phase, P_1 increases with increasing L, while in the spin glass phase P_1 decreases. Finding the value of p where P_1 changes from increasing to decreasing with L will give us a rough idea what the value of p_c is.

We can also use the finite size scaling analysis to get a better value of p_c.

Since 2J excitations come from the spanning paths, they can be treated as a percolation problem. We assume here the scaling relation for P_1 as

$$P_1 L^{\psi} = f[(p - p_c) L^{\phi}], \tag{3.38}$$

in analogy with a percolation threshold [48]. The critical parameters ψ and ϕ, as well as the transition concentration p_c, are chosen to give a good data collapse for all data points. Let us denote (x_{ij}, y_{ij}) as the jth data point of the ith data set. In our case x_{ij} represents the concentration p_j for the system with linear dimension L_i, while y_{ij} represent the corresponding value of $(P_1)_{ij}$. The good data collapse can be obtained by minimizing the quality number S

$$S = \frac{1}{N_d} \sum_{ij} \frac{(y_{ij} - Y_{ij})^2}{dy_{ij}^2 + dY_{ij}^2}, \tag{3.39}$$

where N_d is the number of selected data points, and Y_{ij} and dY_{ij} are the values of the master curve f at point x_{ij} and the corresponding uncertainty, respectively. We can see that the value of S gives the mean square distance to the master curve of the selected data points in the units of standard uncertainties. For a good data collapse, S should be less than or around 1. Note that, since the master curve f is not known and needs to be determined from the data points, we have to include the uncertainties dY_{ij} in the calculation of S above.

To calculate Y_{ij} and its uncertainty, we use the method provided by Houdayer and Hartmann [29]. After applying the scaling law, we select two adjacent points j' and $j' + 1$ around x_{ij} from the set $i' \neq$ i according to the relation $x_{i'j'} \leq x_{ij} \leq x_{i'(j'+1)}$. If there is no pair in the i'th set that satisfies this relation, we will not use the data in the i'th set to calculate the master curve at x_{ij}. If there is no such pair for all data sets i', then Y_{ij} and dY_{ij} are not defined at x_{ij}. The total number of data points that give the master curve is thus N_d.

Once all pairs around x_{ij} are selected, the value of Y_{ij} and its uncertainty dY_{ij} can by calculated using the standard linear least square fitting procedure.

The uncertainties of the critical exponents ψ, ϕ and also the transition concentration p_c, can be obtained using the method described in [10]. We fix one corresponding parameter at various values while optimizing S with respect to the rest.

The range of the fixed parameter that gives S double to the minimum value is defined as the uncertainty.

3.3.2 Uncertainty of the Data Points

We can see in the last section that, to calculate the quality number S, we need to know the uncertainty dY_{ij} of each data point. In principle we have to generate a large number of data sets and evaluate the standard deviation of each data point of P_1. Obviously, this is impractical, if not impossible. We use here the bootstrap method [49,50] to evaluate the uncertainty of each data point. The basic idea of this "quick and dirty" method [50] is that, we use the data set as the best available information of the distribution of itself. By resampling from the original set without replacement, that is, each data point can be resampled more than once, we will have new data sets that reflect the distribution of the original set. The standard deviation of these new sets give us the estimation of the uncertainty of the original data points.

3.3.3 Distributions of Low-Lying states

As the second issue of this thesis, we investigate the distributions of $2J$ and $4J$ states. According to equation 1.4, it is not M_1 and M_2 but M_1/M_0 and M_2/M_0 that contribute to the low temperature specific heat, so we will investigate these ratios instead of directly investigating M_1 and M_2.

For $2J$ states, we expect that the most probable value of M_1 should be zero, since in ferromagnetic phase the $2J$ state vanishes in thermodynamic limit. It is instructive to investigate the cumulative probability C_1, which is defined as

$$C_1(x) = prob\left(\frac{M_1}{M_0} \le x\right). \tag{3.40}$$

Below p_c, we expect that the number of $2J$ states should decrease when L is increasing, and C_1 approaches 1 at all points $x \ge 0$. Above p_c, on the contrary, $2J$ states exist. These spanning $2J$ excitations should share some similarity to the spanning $4J$ excitations. According to [12], we expect that the probability of getting large M_1/M_0 is finite, and C_1 should have a fat tail.

For $4J$ states, we are interested in the probability density function $H_2(x)$, which is defined as

$$H_2(x)\,dx = prob\left(x \le \frac{1}{L^2}\frac{M_2}{M_0} < x + dx\right). \tag{3.41}$$

In the ferromagnetic phase, with low defect concentration, the defected bonds are isolated, as shown on the left of figure 3.2, and we have a unique ground state (aside from global spin flips). The ground state degeneracy M_0 is thus 1. At each defect bond there are two ways to excite the $4J$ states, by flipping one of the two spins joined by the defect bond. Since the total number of bonds is $2N$, there are approximately $2pN$ defect bonds when N is large, and the degeneracy of $4J$ states M_2 is $4pN$. The ratio M_2/M_0per spin is $4p$. We may expect that the probability density $H_2(x)$ should develop a sharp peak at this value when L is increasing.

For the canonical spin glass, $p = 0.5$, it was shown in [12] that the height of $H_2(x)$ collapses with increasing L. This is totally different from the low concentration case described above. We expect that sharpness and collapse of the peak of the probability densities are the characteristics of the ferromagnetic and spin glass phases, respectively. To confirm this, we investigate the behaviour of $H_2(x)$ just above and below p_c to see whether or not they behave very differently as in the cases of low concentration ferromagnetic and canonical spin glass phase.

To get the density $H_2(x)$, we use the kernel density estimation method [51]. The basic idea is that, instead of representing each data point as a rectangular function as in the histogram method, they are represented as a kernel function. The probability density is estimated from

$$\tilde{f}_h(x) = \frac{1}{nh}\sum_{i=1}^{n} K\left(\frac{x - x_i}{h}\right), \tag{3.42}$$

where $K(x)$ is the kernel function, $h > 0$ is the smoothing parameter called bandwidth, and n is total number of data points. The kernel function can be any symmetric function that integrates to one. We can see that the histogram of $\{x_i\}$ can be regarded as a special case of this method with a rectangular kernel function K that satisfies

$$K(x-x_i)=\frac{1}{b_i} \quad \text{if } x \text{ is in the bin that contains } x_i$$
$$=0 \quad \text{otherwise ,} \tag{3.43}$$

where b_i is the width of bin that contains x_i. Note that in this case $h = 1$.

The advantage of this method is that if we choose a suitable kernel, we will get a smooth estimated density which converges to the true density faster than with the histogram method. A commonly used kernel is the standard or unit normal density function which is the Gaussian distribution,

$$K(x)=\frac{1}{\sigma\sqrt{2\pi}}\exp\left[-\frac{(x-\mu)^2}{2\sigma^2}\right], \tag{3.44}$$

with $\mu = 0$ and $\sigma = 1$.

The most important issue is how to choose the appropriate bandwidth. This is similar to the issue of choosing a proper bin width in the histogram method. We adopt here the adaptive algorithm described in [52]. By this algorithm the bandwidths are adjusted due to the local density of the data. This fits our requirement since we expect a fat-tail distribution in the spin glass phase, where the density of data points can be very different around the peak and in the tail.

3.4 Computational Details

We use the algorithm described in section 3.2 to calculate the ratios M_1/M_0 and M_2/M_0. System sizes range from $L = 8$ to 129. Defect concentrations range from $p = 0.050$ to 0.150. Numbers of disorder realisations are 20000 for $L \leq 49$, 10000 for $L \leq 97$, 5000 for $L = 113$, and 2000 for $L = 129$. For each value of L, the number of disorder realisations are the same for all values of p.

We adapt the FORTRAN code used in [12,14]. In these works the system sizes are even, and the lattices have two-colour symmetry, as shown on the left of figure 3.14. The original code takes advantage of this symmetry to reduce the logical test time and memory. In our work some of the system sizes are odd and there is no colour symmetry (see the right part of figure 3.14), so we need to modify the original

code to ignore the symmetry. This results in a slightly longer computing time. The memory issue does not matter since a memory card is very cheap now and a large amount of memory can be easily accessible even though the code is run on a PC.

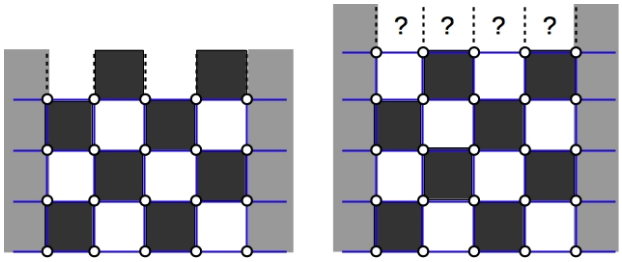

Figure 3.14: (Left) A system with even L in the direction of periodic boundaries (vertical dash lines) having two-colour symmetry. (Right) When L along the direction of periodic boundaries is odd, the colour symmetry is destroyed.

The data for M_1/M_0 and M_2/M_0 were generated on the TERA cluster at Thai National Grid Center (shut down now) and on the Rock cluster at the Department of Physics, Kasetsart University. We used up to 300 nodes in our calculations. The CPU times for a disorder realisation range from a few seconds for the smallest size to almost 24 hours for the largest size. It took about a year to collect all the data used in this work.

The data was then analyzed on four intel Quad-core CPUs. Finite size scaling analysis is performed using the algorithm described in section 3.3.1. We adopt an implementation of this algorithm in the Python language available to be downloaded from [53]. It is straight forward to calculate the cumulative probability of M_1/M_0. To get the probability density function of M_2/M_0, we use a MATLAB implementation on the kernel density estimation [52]. The code is downloadable from [54].

CHAPTER IV
RESULTS AND DISCUSSION

4.1 Transition Concentration

To get a rough idea of the value of the transition concentration, we plot the probability P_1 at various values of system size L and defect concentration p, as shown in figure 4.1. We can see that at the defect concentration below 0.102 the probability P_1 is decreasing with increasing L, and we can say that the system is in the ferromagnetic phase. Above p = 0.106 the probability P_1 is obviously increasing and the system is in the spin glass phase. The transition concentration must lie between these two concentrations.

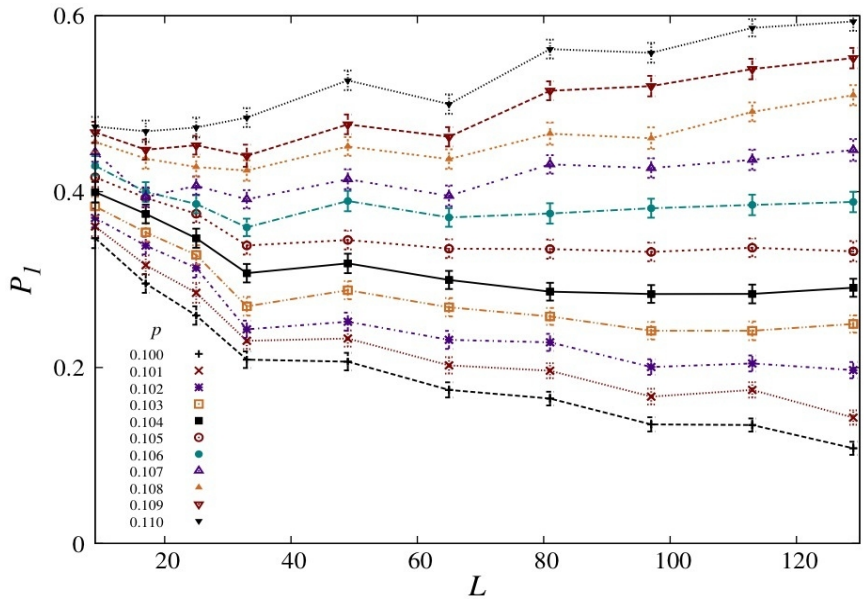

Figure 4.1: The probability P_1 of finding $\frac{M_1}{M_0} > 0$, plotted as a function of system size L for various values of antiferromagnetic bond concentration p.

To get a more precise value of p_c, we perform a scaling plot, as shown in figure 4.2, using equation 3.38. In this plot we fix $\psi = 0$. This is reasonable since the value of P_1 is bounded in the range [0,1]. However we also have tested the

optimisation without ψ fixed. The result gives $\psi < 0.001$.

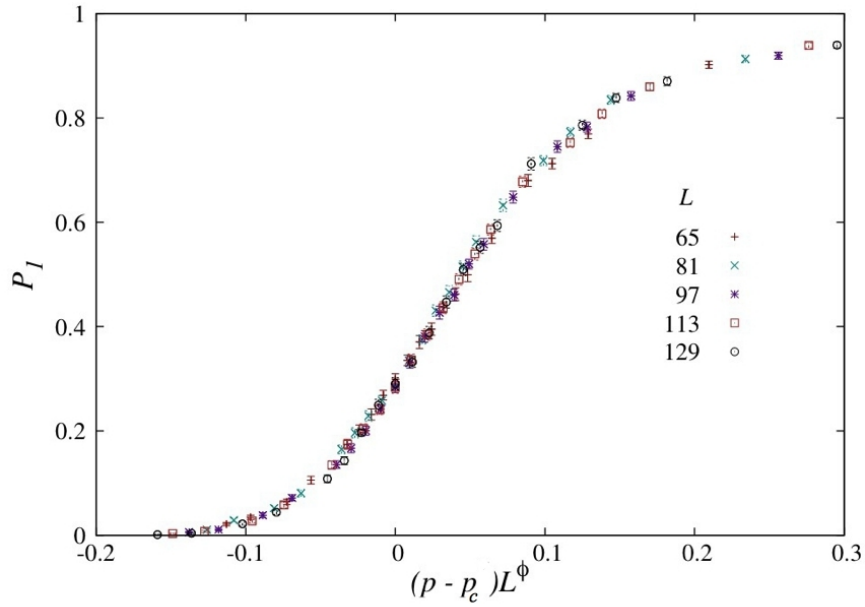

Figure 4.2: The scaling plot of P_1 as a function of the antiferromagnetic bond concentration p with $p_c = 0.1045(11)$ and $\phi = 0.532(72)$.

The scaling plot is quite impressive. The data collapses with the good quality number $S = 0.62$. The optimised values of ϕ and p_c are found to be 0.523(72) and 0.1045(11), respectively. Figure 4.3 gives the variation of the minimised quality number $S_{\min}$ as a function of p_c. The uncertainty of pc can be obtained from this curve, as described in section 3.3.1. The uncertainty of ϕ is obtained in the same fashion.

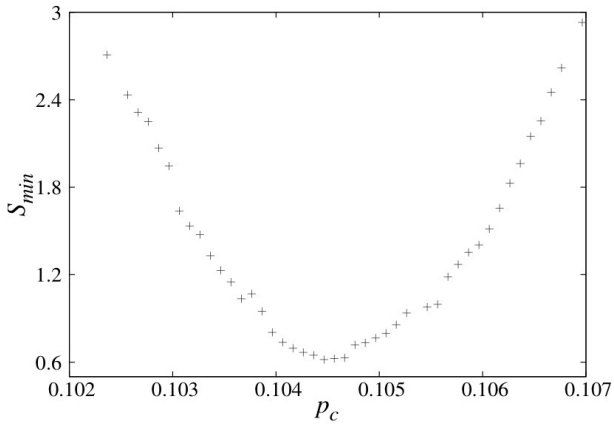

Figure 4.3: The variation of $S_{\min}$ as a function of p_c.

The value of p_c agrees, within error bars, with $p_c = 0.103(1)$ proposed in [10] but disagrees with $p_c = 0.1022(3)$ proposed in [11]. The slightly larger value of our p_c may be due to the finite size effect. We have tested this by performing the analysis using data from systems with $L \leq 65$ and get $p_c \geq 0.105$. This suggests to us that the effect of finite size is an overestimation of p_c. We expect that a smaller value of p_c will be obtained from the analysis of the system with $L > 129$.

4.2 Distributions of Low-Lying States

The results in the previous section confirm our expectation that the transition concentration where P_1 changes from 0 to 1 coincides with the ferromagnetic to spin glass transition. We now go further by looking at the differences of distributions of low-lying states just below and above the transition, at $p = 0.090$ and $p = 0.110$ respectively. Figure 4.4 shows the cumulative probability C_1 of finding $M_1/M_0 \leq x$ for $p = 0.090$. We can see that the most likely value of M_1/M_0 is zero. The probability of getting $M_1/M_0 > 0$ is decreasing with L. We may expect that in the thermodynamic limit, $C_1 = 1$ for any $M_1/M_0 \geq 0$, which means that, in the ferromagnetic phase, the $2J$ states vanish. This result agrees well with the scaling analysis in the previous section.

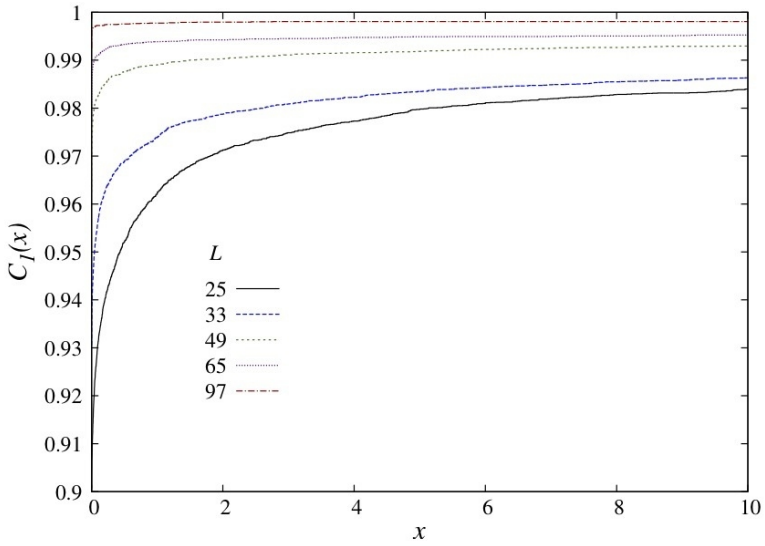

Figure 4.4: The probability $C_1(x)$ of finding $\frac{M_1}{M_0} \leq x$ for $p = 0.090$.

We next look at the distributions of M_1/M_0 just above p_c. Figure 4.5 shows the cumulative probability C_1 of finding $M_1/M_0 \leq x$ for $p = 0.110$. We can see that the most likely value of M_1/M_0 is still at zero. However the probability of getting $M_1/M_0 > 0$ is increasing with L. The distributions of $2J$ states do not develop a sharp peak but broaden when L is increasing. The decreasing of C_1 with L suggests us that, in the spin glass phase, when L is large enough, the $2J$ states will always occur. This again agrees with the scaling analysis. We have from these results that, for the system with odd L, the energy gap in the spin glass phase is $2J$.

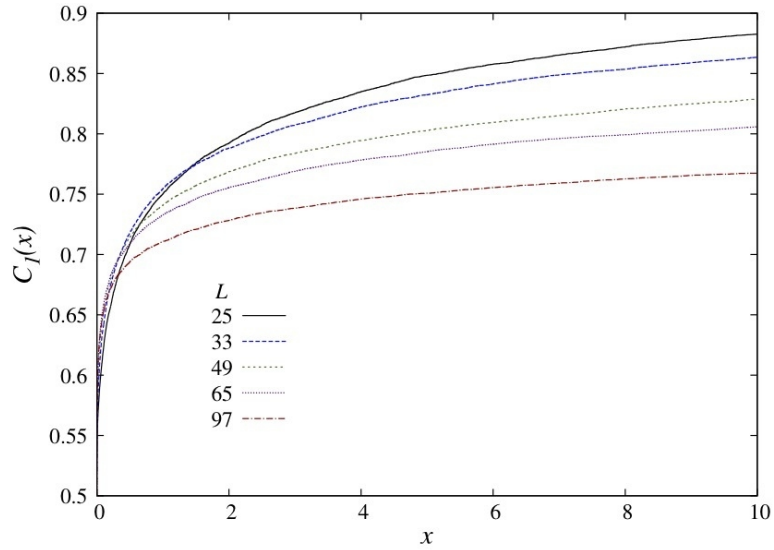

Figure 4.5: The probability $C_1(x)$ of finding $\frac{M_1}{M_0} \leq x$ for $p = 0.110$.

It is naively expected that, according to equation 1.5, the first excited states should dominate the thermal response of the system when the temperature is low enough. We found that this is not the case for our system. Following the trend of C_1 when L is increasing, the ratio M_1/M_0 will not have a definite value in the thermodynamic limit. This sample-to-sample fluctuation of M_1/M_0 gives rise to the same behaviour in the specific heat. This is not what we expect for a physical quantity. When L is large, the specific heat should have a definite value. This depends only on the defect concentration but not on the detailed distribution of the defects. This suggests to us that, even though the energy gap is $2J$ in the system with odd L, it is not physically meaningful to say that the $2J$ excitations dominate the thermal response at low temperature.

We next investigate the distribution of 4*J* states for the systems with odd *L*. Since we expect that, from the above results of C_1, in the ferromagnetic phase the 2*J* states vanish in the thermodynamic limit, the first excited states have energy 4*J*. Figure 4.6 shows the probability density functions H_2 for $p = 0.090$ with various values of odd *L*. We can see a sharp peak develops with increasing *L*. From this trend, we may expect to get a definite value of M_2/M_0 per spin in the thermodynamic limit.

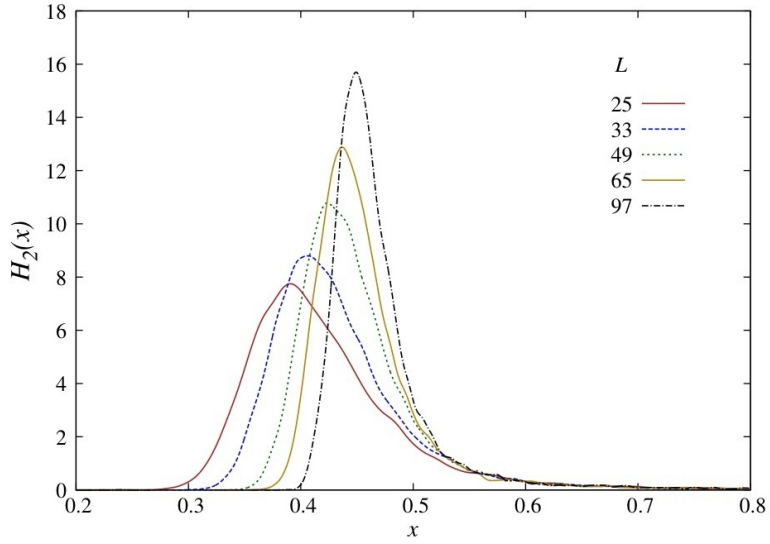

Figure 4.6: The probability density $H_2(x)$ of getting $\frac{1}{L^2}\frac{M_2}{M_0} = x$ for $p = 0.090$ with odd *L*

Since we cannot get 2*J* excitations in the systems with even *L*, the first excited states also have energy 4*J*. Figure 4.7 shows the probability density functions H_2 for $p = 0.090$ with various values of even *L*. We can see we get the same behaviour as in the odd *L* case. We can say that in the ferromagnetic phase, the energy gap is 4*J*, no matter whether we have odd or even *L*. This also suggests to us that we will get a definite value of M_2/M_0 per spin in the thermodynamic limit. According to equation 1.5, the specific heat will have a definite value too.

In the spin glass phase, the behaviour of the 4*J* states is quite different. Figure 4.8 shows the probability density functions H_2 for $p = 0.110$ with various values of odd *L*. We can see that the distribution is collapsing with increasing *L*. The height of the peak is decreasing and the distribution is broadening. The most likely value also

shifts upwards when L is increasing.

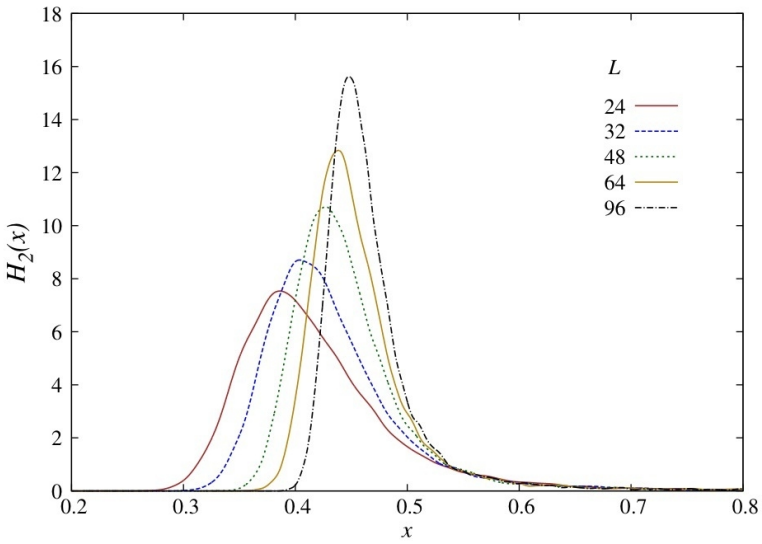

Figure 4.7: The probability density $H_2(x)$ of getting $\frac{1}{L^2}\frac{M_2}{M_0} = x$ for $p = 0.090$ with even L

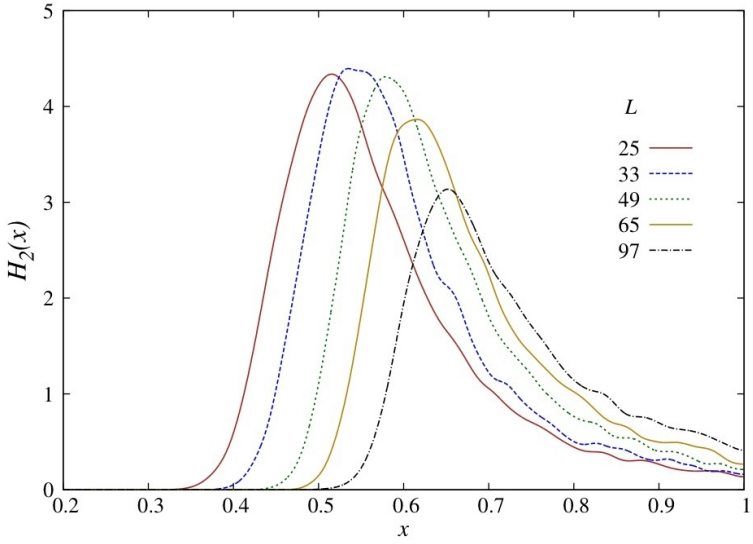

Figure 4.8: The probability density $H_2(x)$ of getting $\frac{1}{L^2}\frac{M_2}{M_0} = x$ for $p = 0.110$ with odd L

The collapsing of the distribution of $4J$ states for the system with odd L is very similar with that of the canonical spin glass model with even L [12]. To see that

this is the behaviour of the spin glass phase, we have investigated the distributions of 4J states for the systems with even L, just above the transition concentration. Figure 4.9 shows the probability density functions H_2 for p = 0.110 with various values of even L. We can see that the distributions are very similar to that of the odd L cases. The collapse of the distribution of 4J states seems to be the characteristic of the spin glass model.

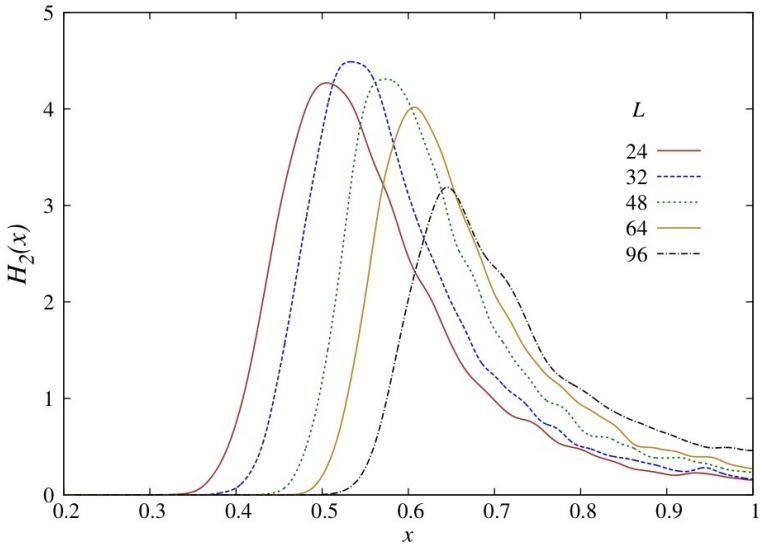

Figure 4.9: The probability density $H_2(x)$ of getting $\frac{1}{L^2}\frac{M_2}{M_0} = x$ for p = 0.110 with even L

For the systems with even L, the first excited states have energy 4J. However, we cannot expect that the low temperature specific heat is dominated by the first excited states. This is due to the sample-to-sample fluctuation, as in the odd L case. It seems to be the characteristic of the spin glass phase that, to get a physically reasonable thermal response, we need the contributions of more energy states than just the first excited states.

CHAPTER V
CONCLUSIONS

We have investigated the existence of spanning $2J$ excitations in the bimodal Ising spin glass model on a square lattice with periodic boundary conditions in one direction, embedded in an infinite ferromagnetic nest in the second direction, and odd L. We find that when the defect concentration is low, the spanning $2J$ excitations are hardly found. In contrast, the spanning $2J$ excitations can be easily found when the concentration is high. By performing the finite size scaling analysis, we found a sharp transition concentration at $p_c = 0.1045(11)$, which, although slightly larger, agrees well with the ferromagnetic to spin glass transition found in the literature. We expect that the discrepancy is due to the finite size effect. This suggests us that, for a system with odd L, the spin glass phase can be characterized by the existence of spanning $2J$ states.

Although we cannot get spanning $2J$ excitations when L is even, we can get the spanning $4J$ paths when the concentration is high enough (see section 3.1). We believe that the spanning excitations are the characteristic of the spin glass phase.

We have also investigated the distributions of low-lying states just above and below p_c. In the ferromagnetic phase, where $p < p_c$, we found that for the system with odd L, the distributions of $2J$ states develop a sharp peak at $M_1/M_0 = 0$ when L is increasing. The probability of finding $M_1/M_0 > 0$ is also decreasing with L. These mean that, although the $2J$ states are possible in the system with odd L, they are hardly found when the system is large. We expect that the $2J$ states are completely absent in the thermodynamic limit.

Since the $2J$ state is not allowed in the systems with even L, we may say that we cannot have $2J$ states in the ferromagnetic phase in the thermodynamic limit, no matter whether the system size L is odd or even. The energy gap is $4J$, independently of L.

We next move to investigate the distributions of $4J$ states in the ferromagnetic phase. Since a $2J$ state is not allowed, $4J$ states are the first excited states. The distributions of M_2/M_0 per spin develop a sharp peak for the systems with both odd and even L. We expect a definite value of M_2/M_0 in the thermodynamic limit. It is reasonable to expect that the thermal response at low temperature is dominated by the first excited states. The low temperature specific heat should have a definite value and follow exponential scaling in the thermodynamic limit.

In the spin glass phase, where $p > p_c$, the behaviour of the distributions of low-lying states are quite different. We found that, for the system with odd L, the distributions of $2J$ states also develop a sharp peak at $M_1/M_0 = 0$ when L is increasing. However, the probability of finding $M_1/M_0 > 0$ is increasing with L. Unlike in the ferromagnetic phase, the $2J$ excitations persist as L increases.

The decreasing of $C_1(x)$ with increasing L indicates that we will not get a definite value of M_1/M_0 in the thermodynamic limit. Even though, in the spin glass phase, the systems with odd L have a $2J$ gap, we cannot expect that $2J$ states dominate the low-temperature thermal response. It is unreasonable to expect a sample-to-sample fluctuation for a physical quantity.

The distributions $H_2(x)$ of the $4J$ states exhibit the same behaviour. We find that they are collapsing with increasing L, for both the systems with odd and even L. This means we cannot expect a definite value of M_2/M_0 per spin even in the thermodynamic limit.

Broadening of the distributions seems to be a characteristic of the spin glass phase. Our results agree well with [12], in which the authors study the distributions of $4J$ states in the canonical spin glass model. This suggests us that we may use the distributions of low-lying states to specify the ferromagnetic to spin glass transition. However, finite size effects prevent us from getting a precise p_c from the data of our available lattice sizes. Finite size scaling analysis is the best way to get the precise value of p_c.

It is interesting to find that, in the spin glass phase, the energy gap is dependent on whether L is odd or even. For odd L the gap is $2J$ while for even L the

gap is 4*J*. However, the difference may not matter. Broad distributions of low-lying states suggests to us that the low temperature behaviour of the system needs contributions from many excited states, not just the first one. We expect that including the contributions of all energy states to the calculation will lead to the definite value of physical quantities in the thermodynamic limit, regardless of the value of the energy gap.

In [13], the authors explain that it is because of the large entropy of the higher excited states that the contributions to the thermal response in the spin glass phase include many excited states, even at low temperature. Our results support this explanation. Collapsing of the distributions of 2*J* and 4*J* states means that a large number of these states can easily be found when *L* is large. It is reasonable to expect an even larger number of higher states can be found. This means that, even though the Boltzmann weights of the higher energy states are small at low temperature, they can be compensated by huge values of degeneracies. Probabilities of finding the higher excited states are comparable to the lower ones. We can thus expect the contributions of many (if not all) excited states to the specific heat.

There are many interesting questions that remain. First, it is interesting to see the contributions of higher excited states to the specific heat. The point is to answer whether or not the specific heat will have a definite value, depending only on the defect concentration but not the detailed distribution of the defect bonds. To answer this question, it is not suitable to work with the periodic-nested boundary conditions used here, since the boundary conditions mimic a defect patch on the infinite ferromagnetic nest. The specific heat obtained will include the effect of the nest. During the time of doing this research we have developed a code for the system with an open boundary. We choose this kind of boundary condition because we can adapt the degenerate state perturbation theory to work with it. The preliminary results show that the distributions of the specific heat have a thiner tail with increasing *L*. However, due to the large computational time to find many excited states (we do the calculations up to the 20^{th} excited states), we can work only with small systems where $L \leq 48$. A faster code is needed to give any conclusion. This line of code development is in progress.

The second question, which is probably more interesting, is the scaling behaviour of the low temperature specific heat. As discussed above, we cannot naively expect exponential scaling. Many works suggest power law scaling, as discussed in chapter 2, where the problem is with the value of the critical exponent α. We are interested to answer this question using our algorithm. The advantage of our method is that we can work at any arbitrary low temperature. It can also be used as a complement to the Monte Carlo method which has problems working at very low temperatures. Our present problem is, however, with the computational time. When L becomes larger we will need more and more excited states involved with our calculation. An optimized code and powerful machines are desperately needed to complete this task.

Apart from the specific heat problem, the spanning path itself is also interesting. As to the third question, it is interesting to investigate the relation between the spanning excitation paths and the collapse of the distributions of low-lying states. Since they are both the characteristics of the spin glass phase, it is reasonable to expect some relation between them. It is also discussed in [12] that the broad distributions of $4J$ states fit well with extreme value statistics. It is very interesting to see how the spanning paths bring this "uncommon" statistic into our system.

As to the last question, we have pointed out above the similarity of spanning excitation paths and domain walls. It is discussed in chapter 2 that there are controversies about fractal dimension of the domain walls. It should be interesting to adapt the technique of entropy difference measurement (equation 2.4) to obtain the fractal dimension of spanning paths, in the hope that this should give some useful information to solve the domain wall issue.

REFERENCES

[1] D. Sherrington. Spin Glasses: A Perspective. In E. Bolthausen and A. Bovier, editors, *Spin Glasses*. Springer-Verlag, Berlin, 2007.

[2] S. F. Edwards and P. W. Anderson. Theory of spin glasses. *Journal of Physics F: Metal Physics*, 5(5):965, 1975.

[3] K. Binder and A. P. Young. Spin glasses: Experimental facts, theoretical concepts, and open questions. *Rev. Mod. Phys.*, 58:801, 1986.

[4] M. Mezard G. Parisi and M. A. Virasoro. *Spin Glass Theory and Beyond*. World Scientific, Singapore, 1987.

[5] A. K. Hartmann and H. Rieger. *Optimization Algorithms in Physics*. Wiley-VCH, Berlin, 2002.

[6] H. Nishimori. *Statistical Physics of Spin Glasses and Information Processing*. Oxford University Press, Oxford, 2001.

[7] J.-P. Bouchaud. The (unfortunate) complexity of the economy. *arXiv:0904.0805*, 2009.

[8] M. Ohzeki and H. Nishimori. Analytical evidence for the absence of spin glass transition on self-dual lattices. *Journal of Physics A: Math.Theor.*, 42(33):332001, 2009.

[9] C. Wang J. Harrington and J. Preskill. Confinement-higgs transition in a disordered gauge theory and the accuracy threshold for quantum memory. *Ann. Phys.*, 303(1):31, 2003.

[10] C. Amoruso and A. K. Hartmann. Domain-wall energies and magnetization of the two-dimensional random-bond Ising model. *Phys. Rev. B*, 70:134425, 2004.

[11] O. Melchert and A. K. Hartmann. Scaling behavior of domain walls at the $T = 0$ ferromagnet to spin-glass transition. *Phys. Rev. B*, 79:184402, 2009.

[12] W Atisattapong and J Poulter. Energy gap of the bimodal two-dimensional Ising spin glass. *New J. Phys*., 10(9):093012, 2008.

[13] C. K. Thomas, D. A. Huse, and A. A. Middleton. Zero- and low-temperature behavior of the two-dimensional $\pm J$ Ising spin glass. *Phys. Rev. Lett*., 107:047203, 2011.

[14] J. A. Blackman and J. Poulter. Gauge-invariant method for the $\pm J$ spin-glass model. *Phys. Rev. B*, 44:4374, 1991.

[15] J-S. Wang and R. H. Swendsen. Low-temperature properties of the $\pm J$ Ising spin glass in two dimensions. *Phys. Rev. B*, 38:4840, 1988.

[16] L. Saul and M. Kardar. Exact integer algorithm for the two-dimensional $\pm J$ Ising spin glass. *Phys. Rev. E*, 48:R3221, 1993.

[17] L. Saul and M. Kardar. The $2D$ $\pm J$ ising spin glass: exact partition functions in polynomial time. *Nucl. Phys B*, 432(3):641, 1994.

[18] J. Lukic, A. Galluccio, E. Marinari, O. C. Martin, and G. Rinaldi. Critical thermodynamics of the two-dimensional $\pm J$ Ising spin glass. *Phys. Rev. Lett*., 92:117202, 2004.

[19] J. Lukic, E. Marinari, and O.C. Martin. Low T scaling in the binary $2D$ spin glass. *Biophysical Chemistry*, 115(23):109 – 114, 2005.

[20] H. G. Katzgraber and L. W. Lee. Correlation length of the two-dimensional Ising spin glass with bimodal interactions. *Phys. Rev. B*, 71:134404, 2005.

[21] J-S. Wang. Worm algorithm for two-dimensional spin glasses. *Phys. Rev. E*, 72:036706, 2005.

[22] H. G. Katzgraber, L. W. Lee, and I. A. Campbell. Nontrivial critical behavior of the free energy in the two-dimensional Ising spin glass with bimodal interactions. *arXiv:cond-mat/0510668*, 2005.

[23] P. Dayal, S. Trebst, S. Wessel, D. Würtz, M. Troyer, S. Sabhapandit, and S. N. Coppersmith. Performance Limitations of Flat-Histogram Methods. *Phys. Rev. Lett*., 92:097201, 2004.

[24] L. de Haan and A. Ferreira. *Extreme Value Theory: An Introduction*. Springer Science+Business Media, LLC, New York, 2006.

[25] T. Jörg, J. Lukic, E. Marinari, and O. C. Martin. Strong universality and algebraic scaling in two-dimensional Ising spin glasses. *Phys. Rev. Lett*., 96:237205, 2006.

[26] G. A. Baker and J. C. Bonner. Scaling behavior at zero-temperature critical points. *Phys. Rev. B*, 12:3741, 1975.

[27] H. G. Katzgraber, L. W. Lee, and I. A. Campbell. Effective critical behavior of the two-dimensional Ising spin glass with bimodal interactions. *Phys. Rev. B*, 75:014412, 2007.

[28] H-F. Cheung and W. L. McMillan. Equilibrium properties of a two-dimensional random Ising model with a continuous distribution of interactions. *J. Phys. C: Solid State Physics*, 16(36):7033, 1983.

[29] J. Houdayer and A. K. Hartmann. Low-temperature behavior of two-dimensional gaussian Ising spin glasses. *Phys. Rev. B*, 70:014418, 2004.

[30] W. L. McMillan. Domain-wall renormalization-group study of the two-dimensional random Ising model. *Phys. Rev. B*, 29:4026, 1984.

[31] W. L. McMillan. Domain-wall renormalization-group study of the three-dimensional random Ising model. *Phys. Rev. B*, 30:476, 1984.

[32] W. L. McMillan. Domain-wall renormalization-group study of the three-dimensional random Ising model at finite temperature. *Phys. Rev. B*, 31:340, 1985.

[33] A. J. Bray and M. A. Moore. Lower critical dimension of Ising spin glasses: a numerical study. *J. Phys. C: Solid State Physics*, 17(18):L463, 1984.

[34] A. J. Bray and M. A. Moore. Critical behavior of the three-dimensional Ising spin glass. *Phys. Rev. B*, 31:631, 1985.

[35] A. J. Bray and M. A. Moore. Chaotic nature of the spin-glass phase. *Phys. Rev. Lett*., 58:57, 1987.

[36] N. Kawashima and H. Rieger. Finite-size scaling analysis of exact ground states for $\pm J$ spin glass models in two dimensions. *EPL (Europhysics Letters)*, 39(1):85, 1997.

[37] D. S. Fisher and D. A. Huse. Equilibrium behavior of the spin-glass ordered phase. *Phys. Rev. B*, 38:386–411, 1988.

[38] D. S. Fisher and D. A. Huse. Ordered phase of short-range Ising spin-glasses. *Phys. Rev. Lett*., 56:1601–1604, 1986.

[39] J. Lukic, E. Marinari, O. C. Martin, and S. Sabatini. Temperature chaos in two-dimensional Ising spin glasses with binary couplings: a further case for universality. *J. of Stat. Mech*., 2006(10):L10001, 2006.

[40] F. Romá, S. Risau-Gusman, A. J. Ramirez-Pastor, F. Nieto, and E. E. Vogel. Influence of the ground-state topology on domain-wall energy in the Edwards-Anderson $\pm J$ spin glass model. *Phys. Rev. B*, 75:020402, 2007.

[41] M. Weigel and D. Johnston. Frustration effects in antiferromagnets on planar random graphs. *Phys. Rev. B*, 76:054408, 2007.

[42] A. Aromsawa and J. Poulter. Domain wall entropy of the bimodal two-dimensional Ising spin glass. *Phys. Rev. B*, 76:064427, 2007.

[43] O. Melchert and A. K. Hartmann. Fractal dimension of domain walls in two-dimensional Ising spin glasses. *Phys. Rev. B*, 76:174411, 2007.

[44] H. S. Green and C. A. Hurst. *Order-Disorder Phenomena*. Interscience, London, 1964.

[45] J. A. Blackman. Two-dimensional frustrated Ising network as an eigenvalue problem. *Phys. Rev. B*, 26:4987–4996, 1982.

[46] J. Poulter and J. A. Blackman. Exact algorithm for spin-correlation functions of the two-dimensional $\pm J$ Ising spin glass in the ground state. *Phys. Rev. B*, 72:104422, 2005.

[47] G. Toulouse. Theory of the frustration effect in spin glasses : I. *Commun. Phys*., 2:99, 1977.

[48] D. Stauffer and A. Aharony. *Introduction to Percolation Theory*. Taylor and Francis, London, 1992.

[49] B. Efron. *The Jackknife, the Bootstrap, and other Resampling Plans*. Society of Industrial and Applied Mathematics, Philadelphia, PA, 1982.

[50] W. H. Press B. P. Flannery S. A. Teukolsky and W. T Vetterling. *Numerical Recipes in Fortran: The Art of Scientific Computing*. Cambridge University Press, Cambridge, UK, 1992.

[51] B. W. Silverman. *Density Estimation for Statistics and Data Analysis*. Chapman & Hall/CRC, London, 1986.

[52] Z. I. Botev, J. F. Grotowski, and D. P. Kroese. Kernel density estimation via diffusion. *Ann.Stat*., 38:2916, 2010.

[53] Melchert O. autoScale.py — a program for automatic finite-size scaling analyses: a users guide. *arXiv:0910.5403v1*, 2009.

[54] Z. Botev. Kernel density estimator — MATLAB Centre. *http://www.mathworks.com/matlabcentral/fileexchange/14034-kernel-density-estimator,* 2007. [Online; access 6-November-2012].

BIOGRAPHY

NAME	Mr. Noparit Jinuntuya
DATE OF BIRTH	17th January 1970
PLACE OF BIRTH	Bangkok, Thailand
INSTITUTIONS ATTENDED	Kasetsat University, 1986-1990 Bachelor of Science (Physics) Kasetsart University, 1991-1995 Master of Science (Physics) Mahidol University, 2007-2012 Doctor of Philosophy (Physics)
RESEARCH GRANTS	Ministry of Science and Technology Thailand, 2007-2011
HOME ADDRESS	261/24 Pahonyothin Rd. Jatujak, Bangkok 10900 Tel. 0817721955 E-mail: fscinpr@ku.ac.th
PUBLICATION	Jinuntuya N. and Poulter J., Elementary excitations and the phase transition in the bimodal Ising spin glass model, *J. Stat. Mech* (2012) P01010.